SUBJECT: **Descriptions of CODEV and APART models of FIRST-SPIRE**

PREPARED BY: **A G Richards**

KEYWORDS: **CODEV, APART, structure**

COMMENTS: **This document describes the present working CODEV model of SPIRE(formerly BOL) and the structural additions made to it in order to generate a realistic APART model suitable for initial thermal radiative transfer and loading computations.**

DISTRIBUTION

A. Richards (RAL)
M Caldwell (RAL)
B.Swinyard (RAL)
M.Griffin (QMW)
Project Office (RAL)

CONTENTS

1. SCOPE

This note is intended to provide a guide to the optical performance of the present SPIRE CODEV optical design and to indicate how the optical design interfaces with those non-optical components which are going to be important in determining thermal background. It is intended to supplement an earlier note, BOL/RAL/N0021 'Straylight analysis - PHOT' dated 20-11-97, by addressing those areas flagged as uncertain or TBD in that note.

2. INTRODUCTION

The details of the FIRST telescope design, for example the primary mirror hole size and the cryostat structure between the rear of the FIRST primary mirror and the SPIRE instrument, have been taken from fairly old and possibly out-of-date project documents. There exist no details of the secondary mirror's support strut geometry. It is therefore important to realise that, where the SPIRE FOV passes close to telescope parts and cryostat infra-structure, these areas will require continuous monitoring as the design process for these structures proceeds in order to catch changes which may lead to optically unacceptable effects on SPIRE as early as possible so that remedies can be proposed.

Given the present definition of the SPIRE optical design, an attempt has been made at representing those structural surfaces and apertures which will surround the optical beam defined by the FOV of the SPIRE detector(s). These surfaces and apertures will be most important in defining the sources and transfer of infra-red radiation which, without prophylactic treatment, may compromise the performance of the SPIRE instrument. The geometry of these surfaces has been determined (or guessed in the case of telescope support struts) and organised into forms suitable for input to the analysis program APART. The APART model of SPIRE is later illustrated. Some initial analyses of thermal radiation loading onto major SPIRE apertures (e.g. '4K' and '2K' filters) have been carried out using APART, but the results will be presented elsewhere.

3. ILLUSTRATING THE PRESENT CODEV DESIGN

A full annotated listing of the major CODEV .SEQ files used to define and ray-trace the present FIRST-SPIRE optical design can be found in section 10.0.

3.1 Raytracing from the FIRST telescope object space to the SPIRE detector

Figure 1 shows an isometric plot of the SPIRE optics when traced with rays which begin in the object space of the FIRST telescope from a direction which corresponds to the axial view of the SPIRE instrument. The principal ray from this direction, at the point where it enters the SPIRE instrument, is inclined at an angle = 2.19894 degrees to the FIRST telescope axis of symmetry and it is located in the YZ-plane of the telescope. Rays from this central field point are traced through to the detector and the effect of tilting the so-called 'chopper mirror' (the second optic in the SPIRE optical train) over an angular range of +- 3.964 degrees is clearly shown. The rotation of the chopper is such as to tilt the rays out of the fold plane of the SPIRE optical train, so that the 'central' field point is tracked from one side of the detector to the other, passing through the centre of the detector on the

way, as is clearly shown in figure 1. The importance of the number 3.964 degrees will be better illustrated when raytracing from the detector outwards is described later.

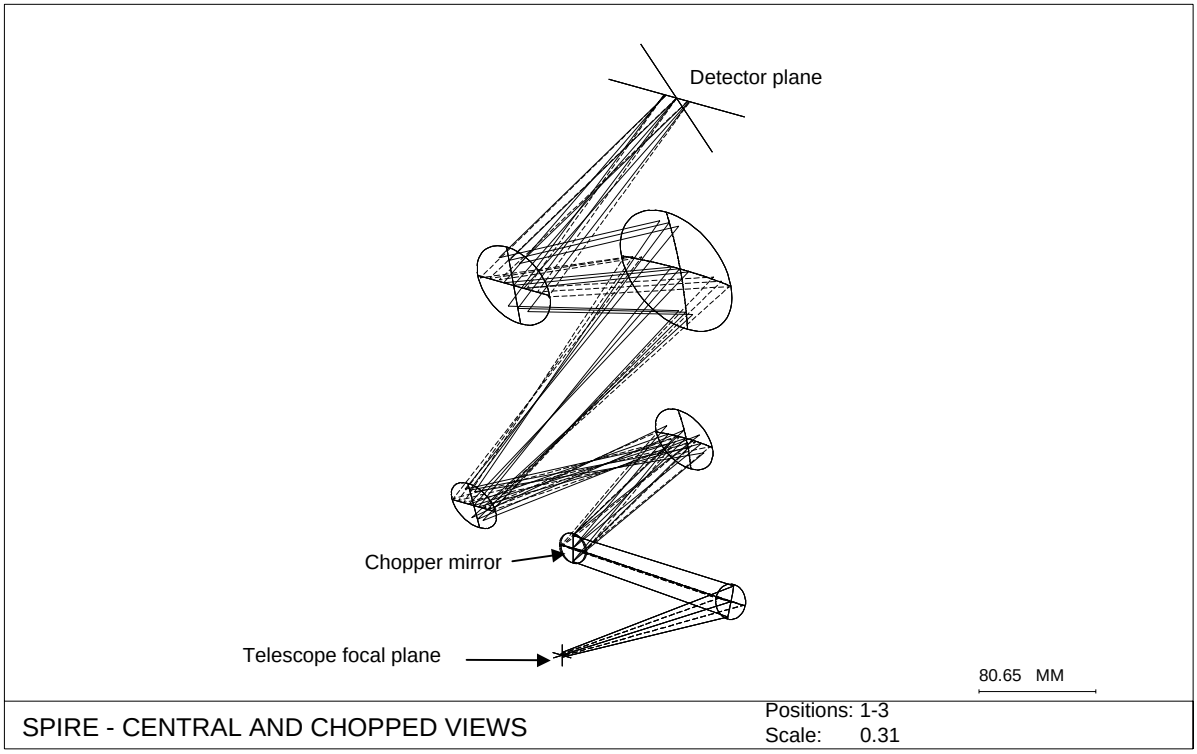

Figure 1 CODEV plot of SPIRE's axial FOV point traced from telescope focal plane to detector, showing the effect of the tilting of the chopper mirror

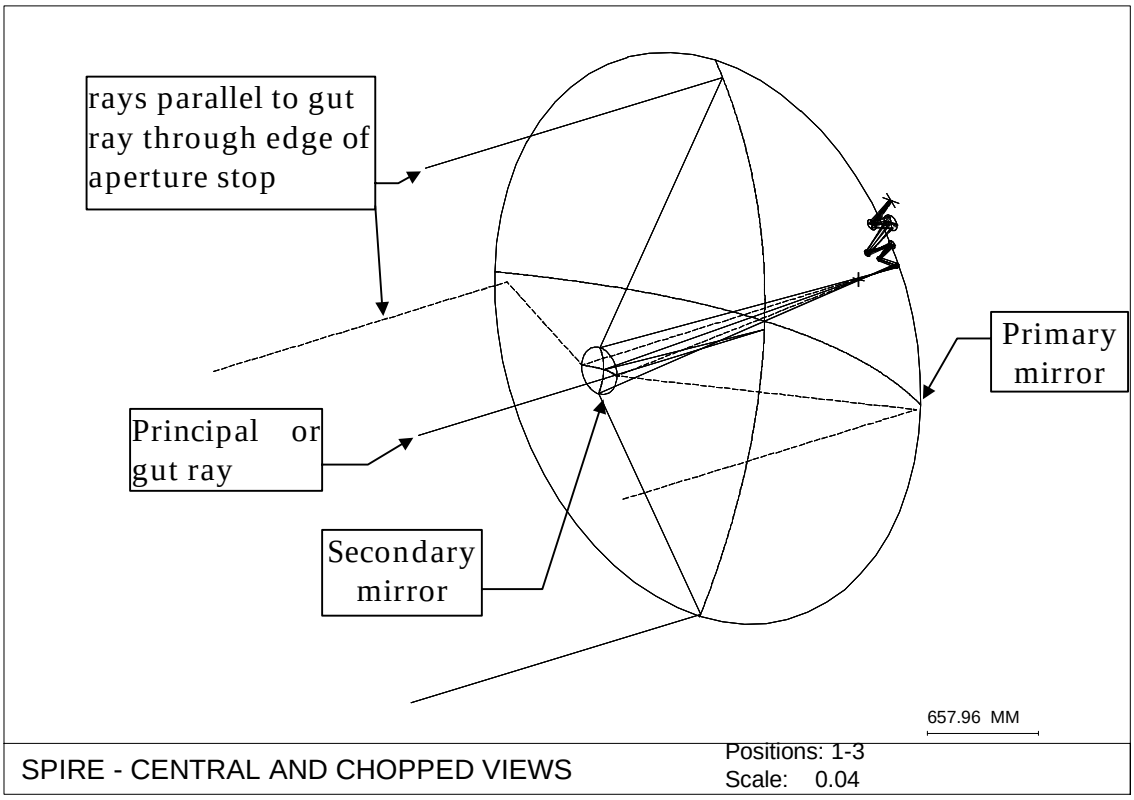

Figure 2 A view of FIRST-SPIRE showing the ray-trace of SPIRE's 'central' view

The telescope aperture stop is located at the secondary mirror of the telescope and figure 2 clearly shows those rays which trace through four points on the edge of the aperture stop. These four rays, together with the principal or 'gut' ray, become the rays shown defining the optical beam in figure 1 when traced onwards. Figure 3 is a YZ-plane section through the plot shown in isometric projection in figure 2, and it is intended to show the gut ray traced through the centre of the secondary (this ray will not physically exist in practice because the secondary will block it). As previously stated, the angular offset between the SPIRE 'axial view' and the axis of symmetry of the FIRST telescope is 2.19894 degrees when measured at the SPIRE aperture, but the input angle at the telescope between the gut ray for this view and the telescope axis is only 0.18290 degrees, or 10.974 arc-minutes. Thus, the SPIRE FOV is offset by 0.1829 degrees from the centre of the telescope's FOV. The principal optical parameters of the FIRST telescope which are used in the present optical design are listed in table 1.

Table 1 Optical design parameters of the FIRST telescope mirrors

Parameter	Primary	Secondary
Radius of curvature	3046.246 mm	267.82995 mm
Conic constant	-1.00 (parabola)	-1.238772 (hyperbola)
spacing	-	1396.3648 mm
Entrance pupil diameter		280 mm

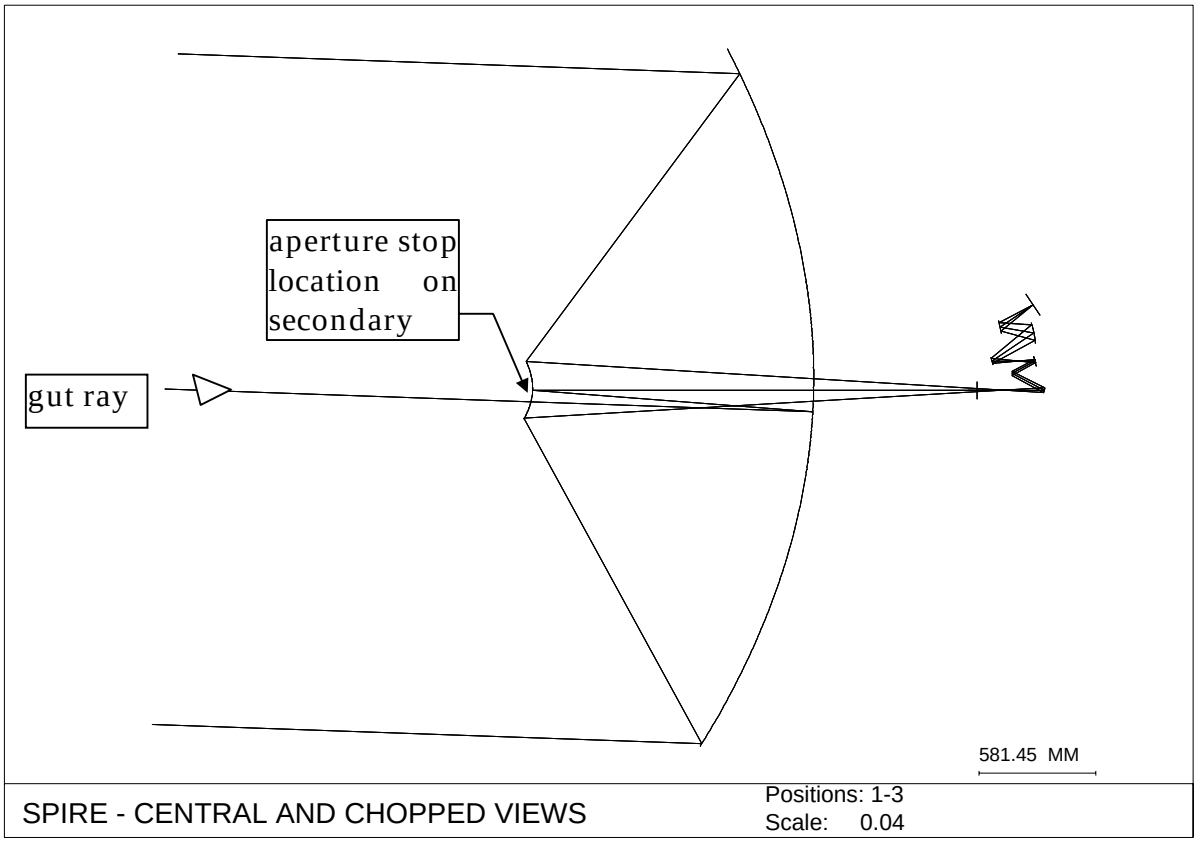

Figure 3 YZ plot of the SPIRE axial view traced from the FIRST telescope object space

3.2 Raytracing from the SPIRE detectors to the FIRST telescope object space

The CODEV design presently shows only one of the three detectors to which the radiation entering the SPIRE FOV will be sent, using flat dichroic beam-splitters to separate the three wavebands centred on 250μ, 350μ and 480μ. Each waveband will have its own detector and the detector formats listed in the SPIRE proposal to ESA are shown in table 2.

Table 2 Proposed detector formats for SPIRE

waveband	pixel size, mm	pixel format	detector size, mm*mm
250μ	0.625	32*32	20*20
350μ	0.875	24*24	21*21
480μ	1.200	16*16	19.2*19.2

Being the biggest, the 350μ detector will define the biggest geometric FOV. In order to determine the FOV that a particular detector will have when projected onto the sky, it is necessary to trace rays in the reverse of the usual direction. This requires generating a CODEV model which is an exact reverse of the model illustrated in the previous sections. This process of generating a reversed system is aided by the CODEV 'flip' command, but there are pitfalls and bugs which must be avoided by careful checking using subsequent

raytracing of the flipped system and comparison with angles of incidence obtained during raytracing of the original unflipped system. In this way an accurate representation of a reversed system has been determined and raytracing outwards from a detector having the largest size shown in table 2 has been carried out. Some results are shown in figures 4 and 5, which are MATHCAD plots of data extracted from CODEV .LIS files of ray co-ordinate data obtained by tracing principal rays from the centre and four corners of the square-format detector (these are rays which pass through the centre of the aperture stop). The ray-tracing was carried out for three angles for the chopper mirror, -3.964, 0.0 and + 3.964 degrees rotation.

Figure 4 shows the views on the sky of the 21 mm square 350μ detector with the chopper mirror rotated by + and - 3.964 degrees from its central position. The boundaries of the two fields of view do not overlap, as required, but they are separated by only about 0.1 arc minutes at their closest points. This indicates that the 3.964 degree chop is presently about the minimum needed to get completely separate views of the sky at the extremes of the chop. The edge of the telescope's 15 arc minute radius unvignetted FOV is indicated. Note that even though the rays shown in figure 4 fall inside the telescope's unvignetted FOV, this does not prove that the SPIRE beam is not vignetted. Whether this is so will depend on the SPIRE aperture stop size and its projection onto the FIRST secondary mirror.

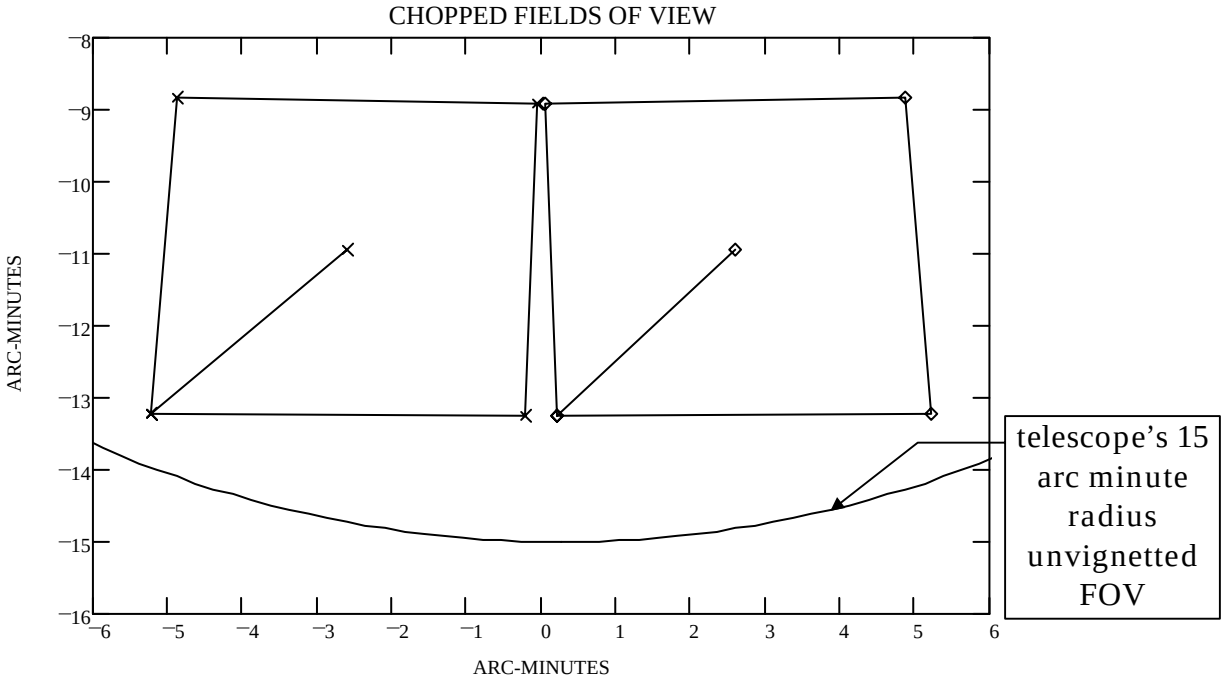

Figure 4 Plot of the 350μ detector's chopped views on the sky

Figure 5 shows (solid line) the detector FOV projected onto the sky with zero chop. Superimposed in dashed outline is a 4.4 arc minute square FOV. This is the size stated for the SPIRE FOV in the document summarising the BOL design produced by ROE. Note how the largest detector FOV exceeds 4.4 arc minutes in the X-direction (horizontal). Note also that the ESA proposal states that SPIRE will have a 4 arc minute square FOV, so in

order to marry up the FOV stated in the ESA proposal with the actual CODEV design, either a 10 % reduction in detector size (20 % in area) or a 10 % increase in overall focal length is required. A focal length change will require changes to the figures of one or more optical surfaces. The data on which figures 4 and 5 are based is presented in table 3.

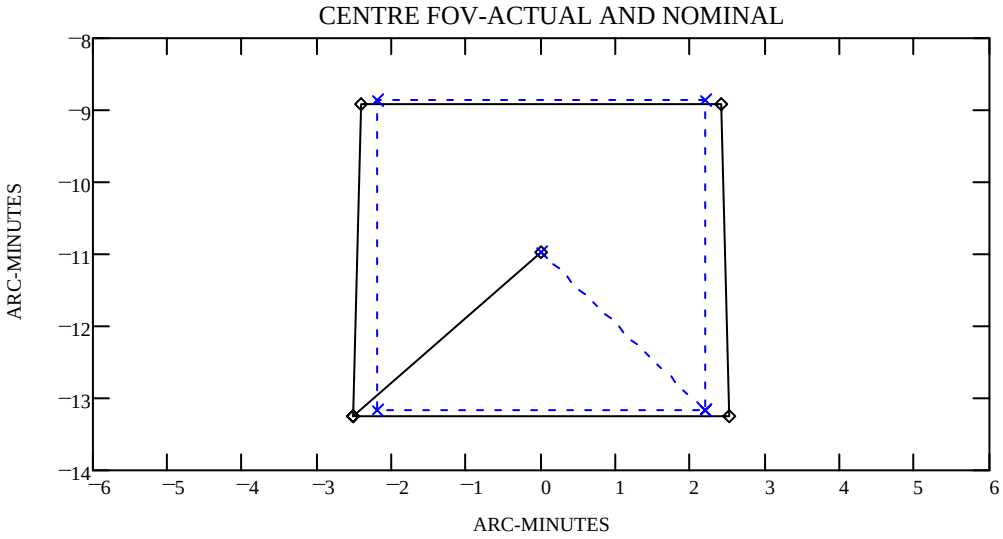

Figure 5 Actual (solid) and proposed (dashed) SPIRE detector fields of view

Table 3 Angles on the sky defining centres and corners of the chopped fields of view

Chop angle (degrees)	X-angle on sky (arc minutes)	Y-angle on sky (arc minutes)	location on detector
-3.964	2.6	-10.96	centre
-3.964	0.2138	-13.26	corner
-3.964	5.214	-13.22	corner
-3.964	4.87	-8.846	corner
-3.964	0.05294	-8.927	corner
0	0	-10.97	centre
0	-2.508	-13.25	corner
0	2.508	-13.25	corner
0	2.416	-8.908	corner
0	-2.416	-8.908	corner
3.964	-2.6	-10.96	centre
3.964	-5.214	-13.22	corner
3.964	-0.2138	-13.26	corner
3.964	-0.05294	-8.927	corner
3.964	-4.87	-8.846	corner

Having generated a ‘reversed’ CODEV model for the combined FIRST-SPIRE optical system, it was used to produce ‘footprints’ of the beam defined by the detector’s view through the SPIRE aperture stop at various locations in the optical system, so that optical components, apertures and structures in and surrounding the optical train could be correctly sized to ensure their edges are clear of the geometrical beam.

4. SIZING COMPONENTS AND APERTURES

Figure 6 shows a schematic (not to scale) layout proposed for the SPIRE bolometer, showing the major optical components and apertures. The philosophy is to compartmentalise the optics into separate temperature regions connecting the detector modules, which must be held at the coldest temperature (around 0.3°K), and the structure nearest to the telescope focal plane, which will probably reach about 9-15°K. In between these two temperature environments will be at least two enclosures, labelled the 2K-box and the 4K box which, as their names imply, are intended to provide stable temperatures for those surfaces defining them at about 2°K and 4°K respectively. There may also be third enclosure or plate, tentatively labelled '1K box'.

Major accommodation constraints on the input side of the SPIRE enclosure are

- at the telescope focal plane, the SPIRE optical axis is specified to be 91 mm from the telescope axis.

- the side of the enclosure nearest the telescope axis can be no nearer than 40 mm to the axis

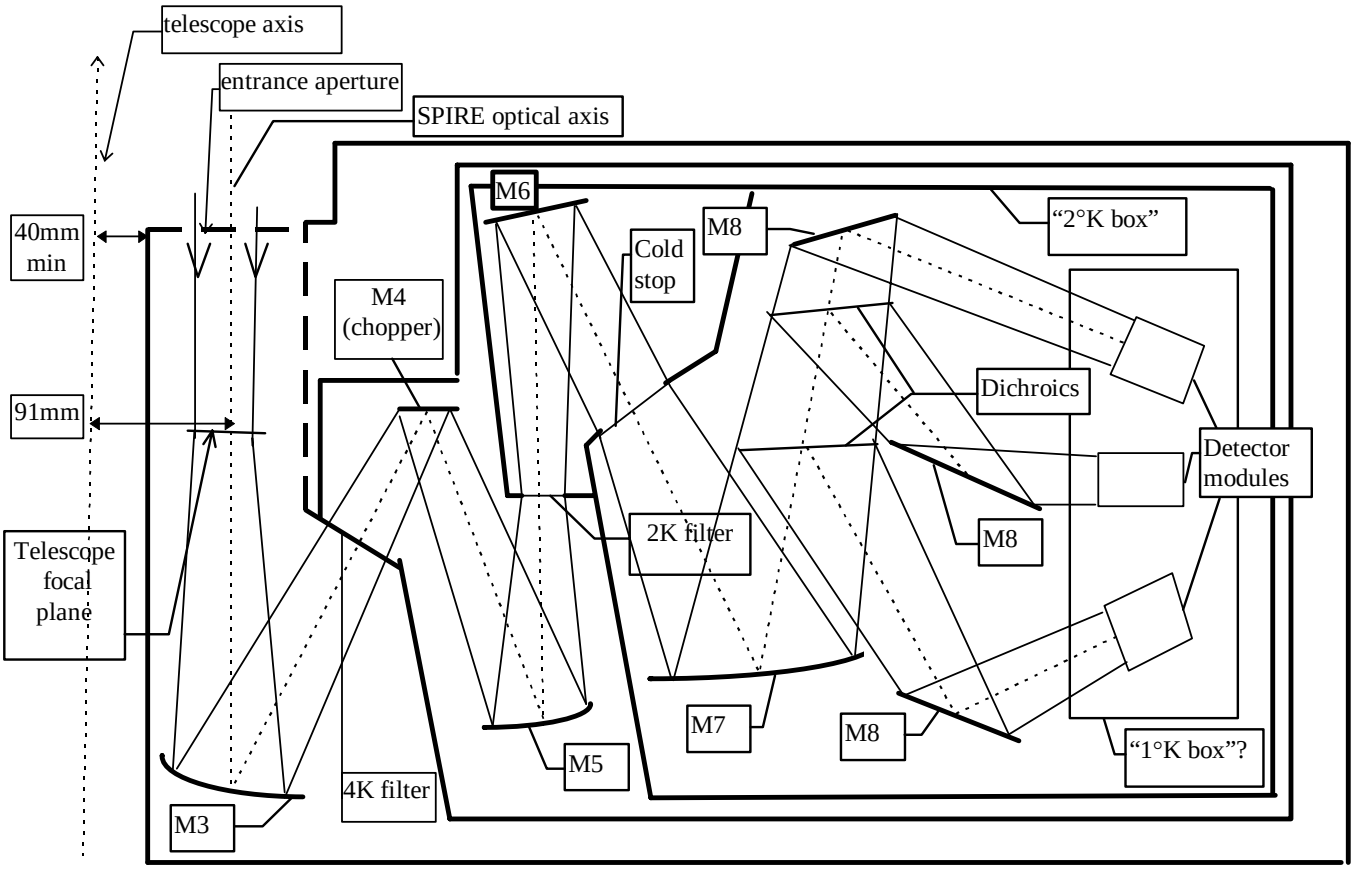

Figure 6 SPIRE layout showing main optics and temperature compartments

The 'window' into the 4K box will be located between M3 and the chopper mirror M4 and a thermal filter (the '4K filter') will be located there to intercept all of the out-of band thermal radiation originating from all surfaces forward of it. The 'window' into the 2K box will be located between M5 and M6 and a thermal filter (the '2K filter') will be located there to intercept all of the out-of band thermal radiation falling onto it from the 4K enclosure. The 2K filter is located at the position of an image of the telescope focal plane formed by M3 and M5.

The optical position chosen for the SPIRE system aperture stop is within the 2K enclosure. This is the 'cold stop' and is therefore the aperture which, taken together with the detector, defines the beam which must be transmitted by all other apertures and optics without vignetting. This beam must also be kept clear of 'warmer' structure in the telescope/cryostat space. Note that components and apertures from the chopper mirror M4 outwards towards the telescope must be sized to include the effect of scanning the chopper mirror between its extreme positions and the composite FOV beam includes this.

Figure 7 shows a schematic layout for the main cryostat and telescope surfaces, indicating the locations external to the SPIRE instrument where the SPIRE optical beam footprint must be closely monitored to ensure clearance. The main places to pay attention to are the hole in the primary and the apertures inside the cryostat cavity and shield through which the focal plane instruments view the secondary mirror and, by reflection from the latter and the primary mirror, support struts and space. Dimensions for circular openings are indicated, the numbers being taken from early FIRST documents. **These numbers and all computations carried out using them may have to be corrected if they are changed during the design process.**

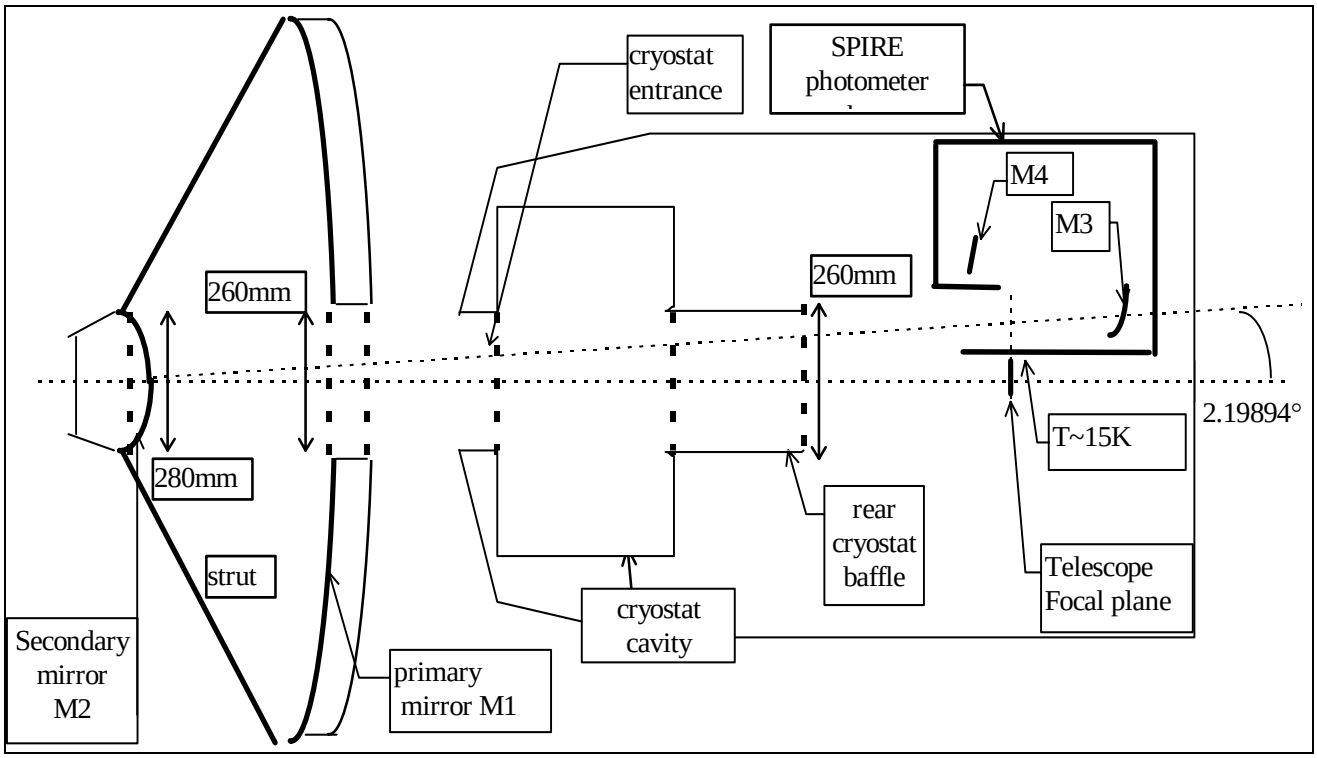

Figure 7 Main external locations where beam clearance must be positive

4.1 Sizing the cold stop

Given the detector size and format, the beam defining the view that the SPIRE detector has of space should be limited only by the cold stop located inside the 2K box in figure 6. In particular, the SPIRE FOV should not be vignetted by the telescope secondary mirror and this was the first place where the SPIRE beam footprint was studied.

4.1.1 SPIRE FOV Footprint at the secondary

Figure 8 shows the composite 'footprint' on the 140 mm radius secondary mirror of the SPIRE FOV produced by projecting rays from the centre and eight points around the edge of the biggest-format detector through an elliptical cold stop having the dimensions shown in the figure and repeated in table 4. The footprint is that on the actual curved secondary surface.

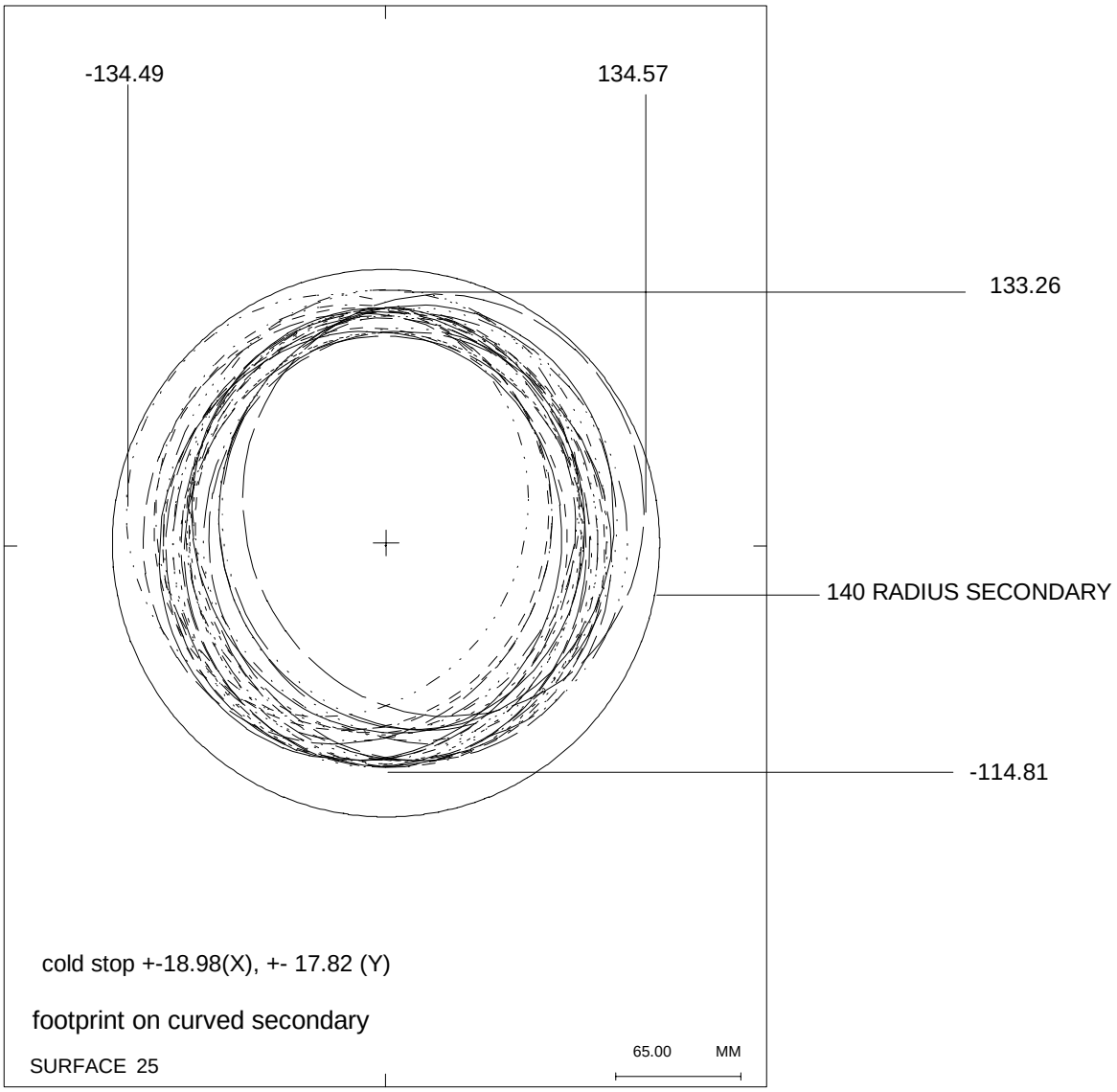

Figure 8 SPIRE FOV footprint on telescope secondary mirror

Figure 8 shows that the present dimension chosen for the cold stop gives no margin at the secondary for SPIRE misalignment tolerances or diffraction effects, so the size given in table 4 and used hereafter is an absolute maximum size permitted.

Table 4 Dimension of an elliptical cold stop used in SPIRE footprint analyses

Dimension	full axis length,mm
X	18.98
Y	17.82

After having set up the cold stop in the CODEV model to have the dimensions shown in table 4, the composite FOV beam was tracked through the optical system and its footprint

on optical surfaces or at apertures was determined and used to size the surfaces and apertures.

4.2 Clearances at the primary mirror hole

Figures 9 and 10 show the SPIRE FOV footprint at the locations of both ends of the hole in the primary mirror. The latter has been taken to be cylindrical with radius 130 mm, the dimension being taken from early FIRST documents.

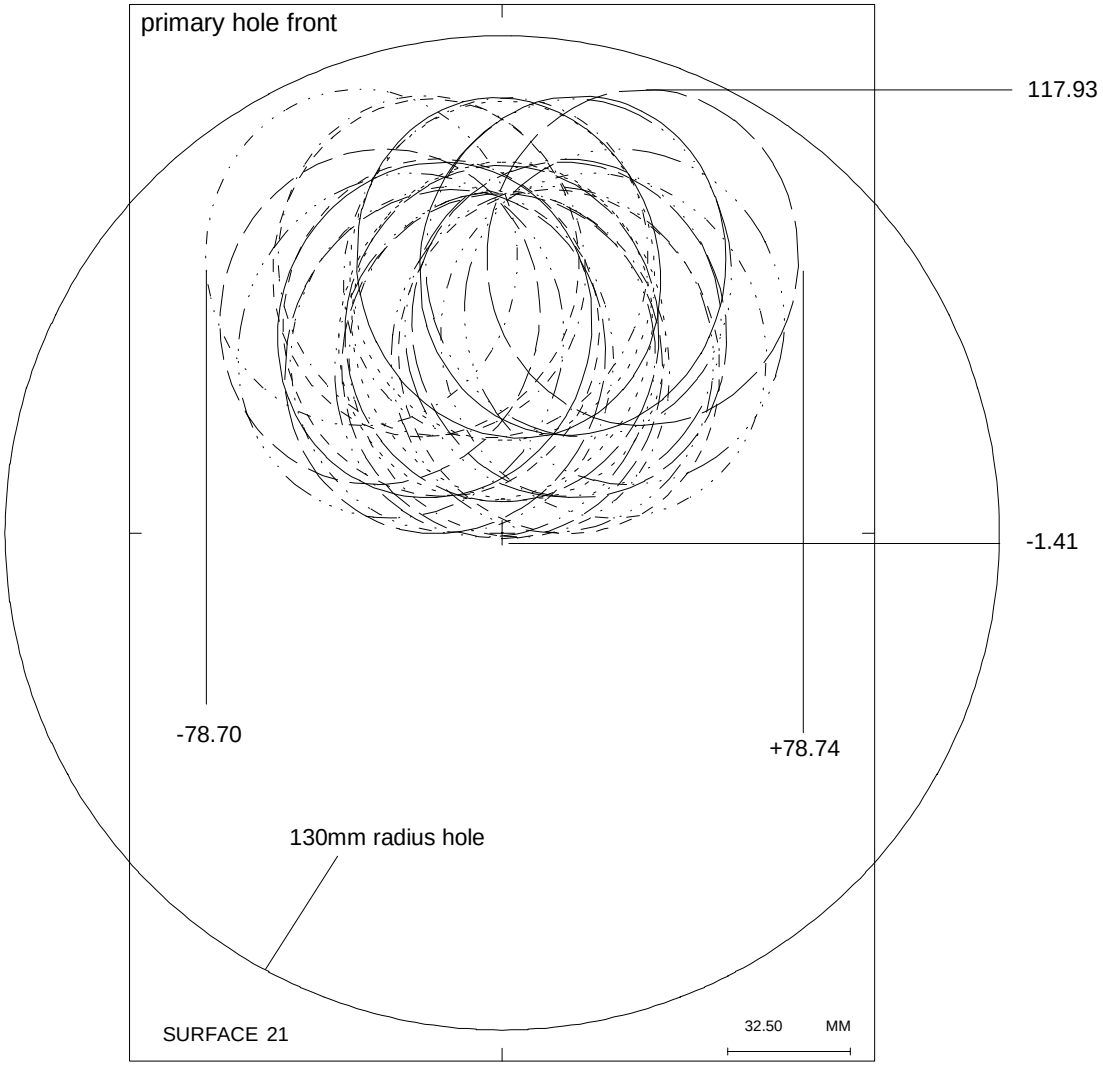

Figure 9 SPIRE FOV footprint at front of primary hole

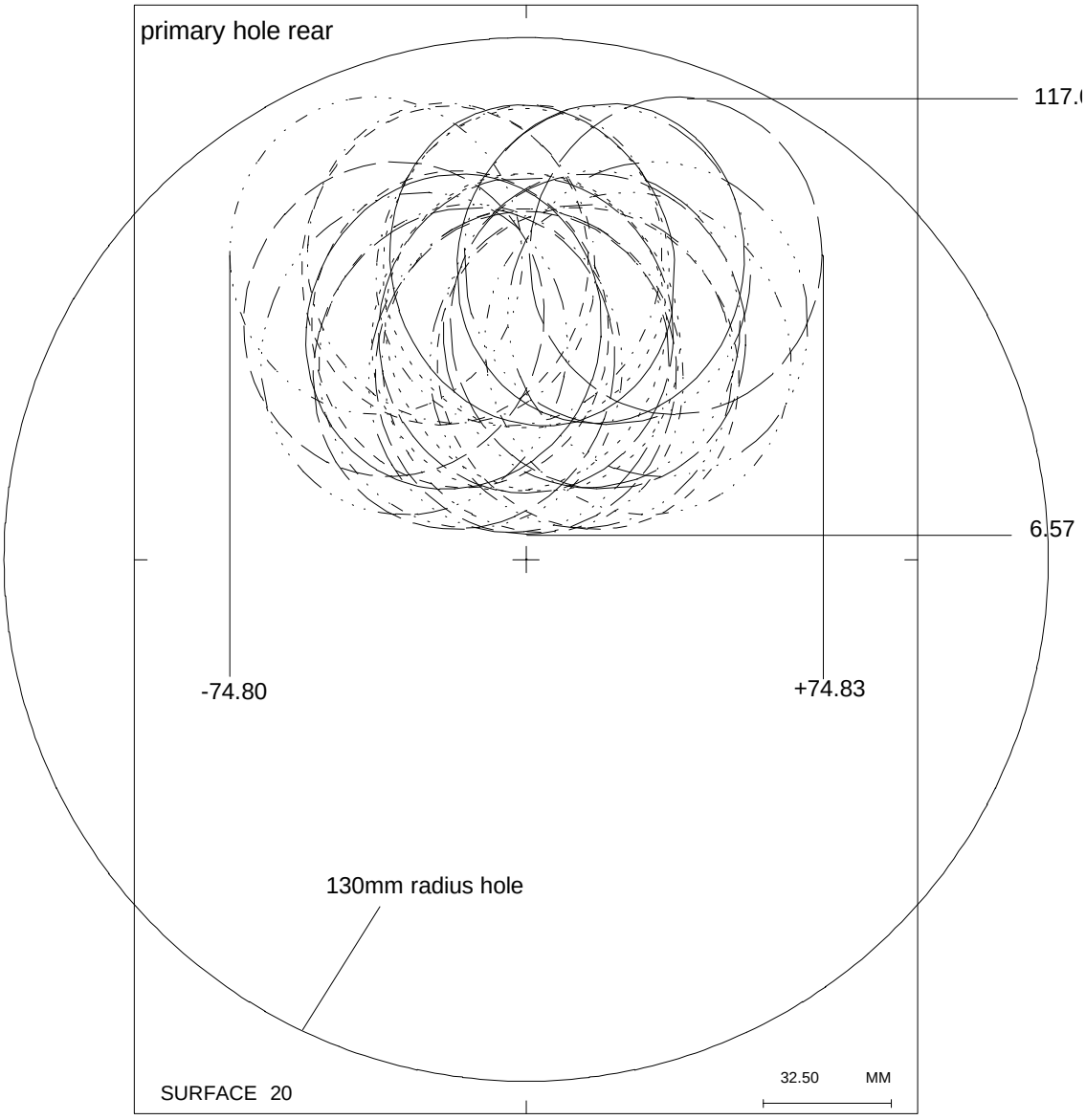

Figure 10 SPIRE FOV footprint at rear of primary hole

4.3 Clearances inside the cryostat

Figures 11, 12 and 13 show the SPIRE FOV footprint at the locations inside the cryostat indicated in figure 7. The internal cryostat apertures have all been set to be 130 mm radius circles concentric with the FIRST telescope's axis of symmetry. As one progresses back along the beam from the telescope through the cryostat towards the entrance aperture of SPIRE, the separate beams belonging to each of the nine field points on the detector (three rows of three points in a square array) begin to be distinguishable and are clearly visible in figure 13. Taking figures 9 to 13 together one can see that the composite beam clearance is smallest at two particular points at the corners of the FOV projected at the two extreme positions for the chopper mirror.

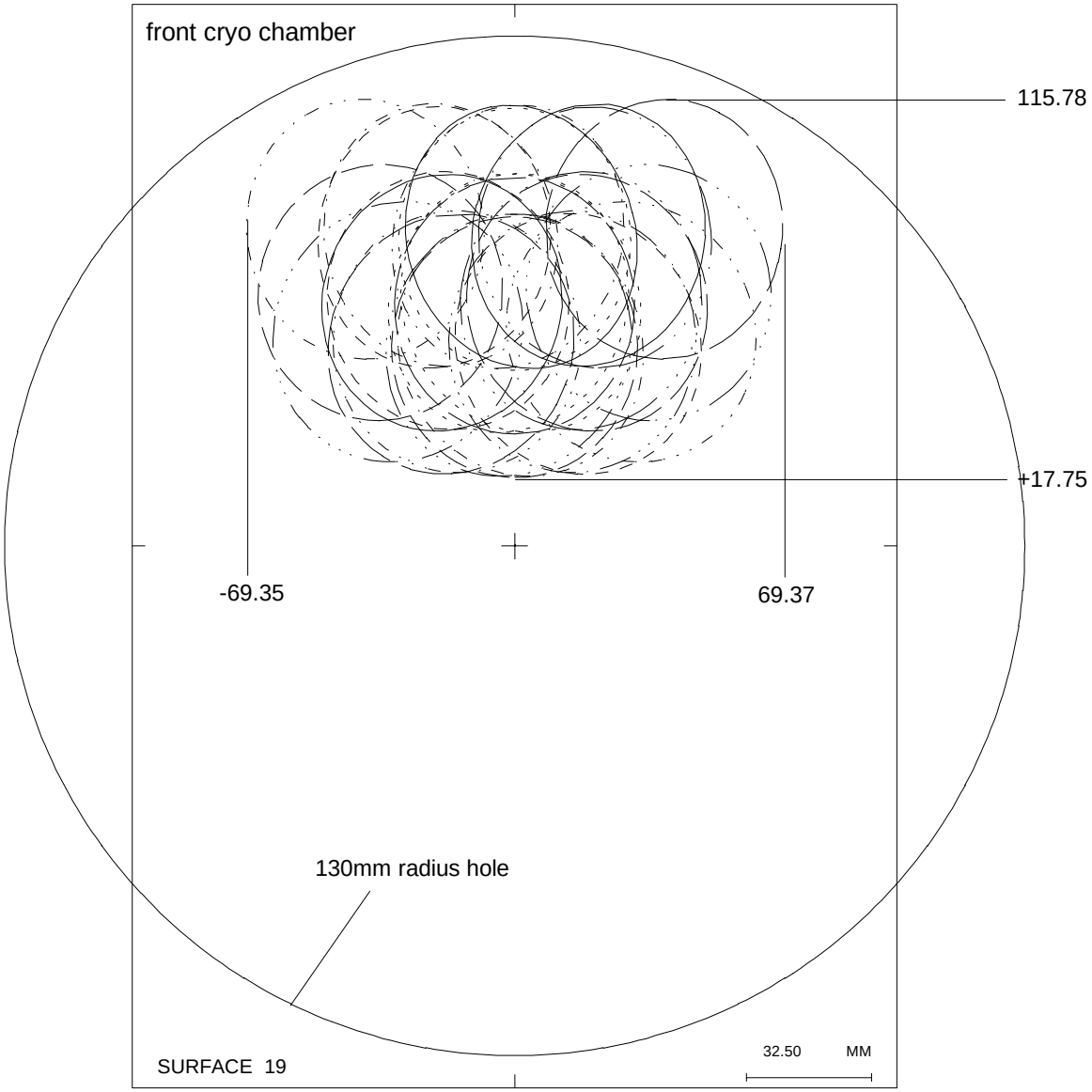

Figure 11 SPIRE FOV footprint at front of cryostat-cavity

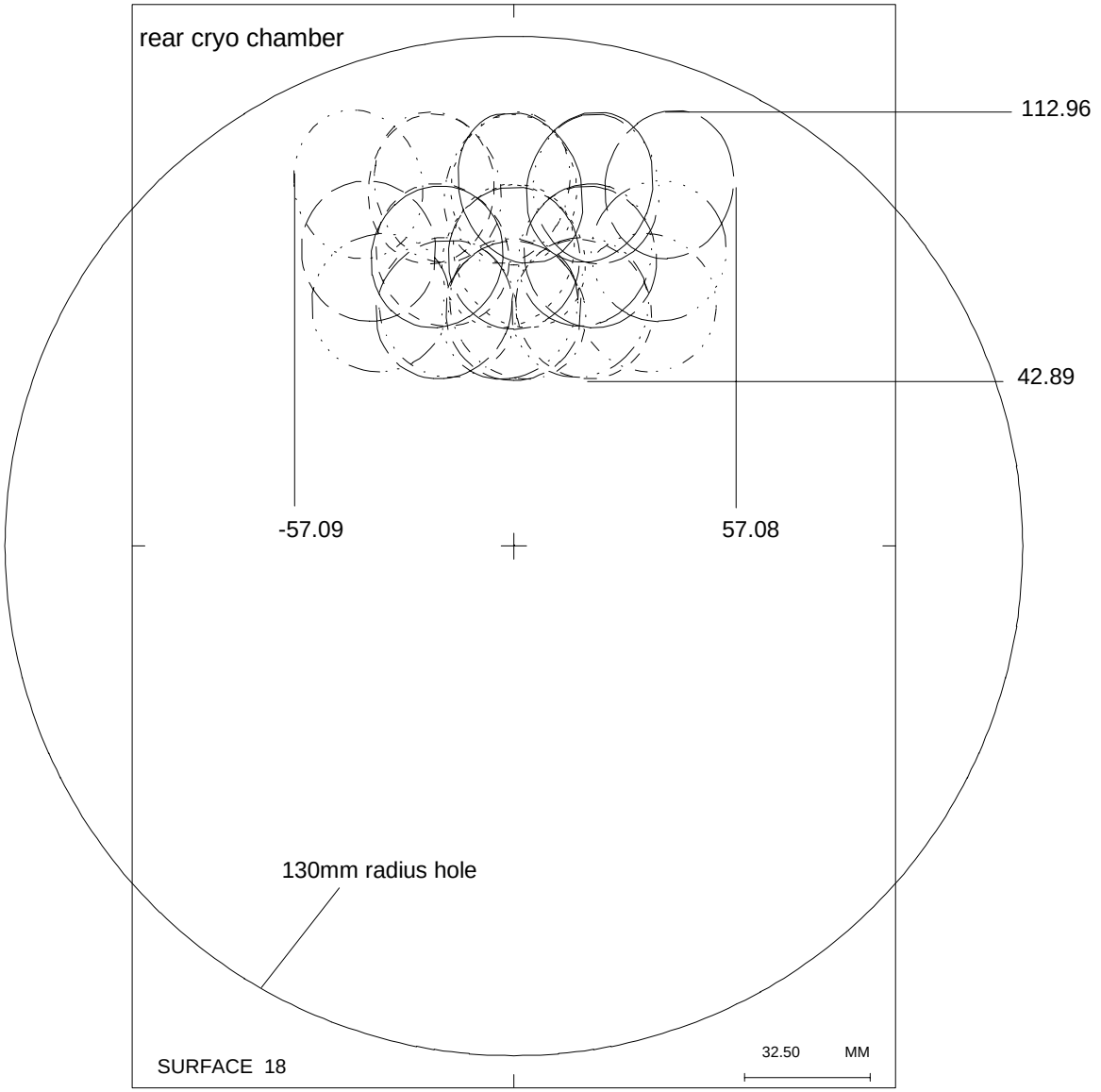

Figure 12 SPIRE FOV footprint at rear of cryostat cavity

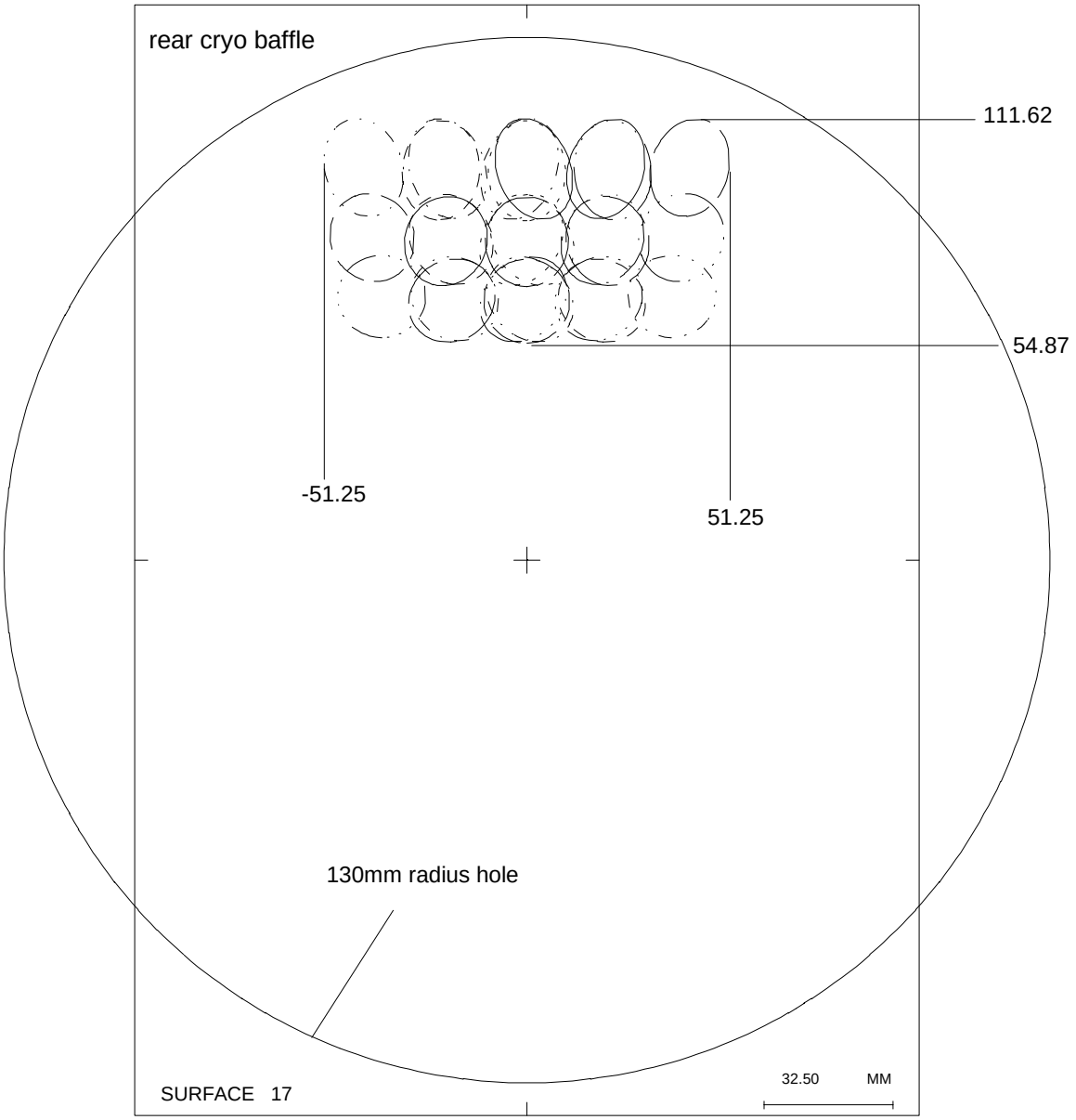

Figure 13 SPIRE FOV footprint at rear of cryostat baffle nearest SPIRE

4.4 Sizing apertures and components inside SPIRE

The next stage is to determine beam footprints at various locations within the SPIRE instrument, starting at a position designated the 'entrance aperture' (see figures 6 and 14). This aperture may or may not be feasible, depending on accommodation restrictions as yet to be finalised. However, at present it will be assumed that, on the telescope axis side of the instrument, the main structure of the SPIRE envelope can be extended forwards to this plane. This aperture plane is presently placed 164.4 mm forwards of the telescope focal plane measured in a direction parallel to the telescope axis. or 164.4/cos(2.19894) when measured in the direction of the principal ray through the centre of the SPIRE FOV. The optical design with the SPIRE optical axis inclined at 2.19894 degrees to the telescope axis puts the centre of the SPIRE FOV at 91 mm from the telescope axis at the level of the telescope focal plane. The outer wall of the SPIRE enclosure, nearest to the telescope axis, is restricted to being no closer than 40 mm to the telescope axis and is therefore best designed to be parallel to the telescope axis in the sectional view shown in figure 6 and displaced sideways by this amount (see figure 14).

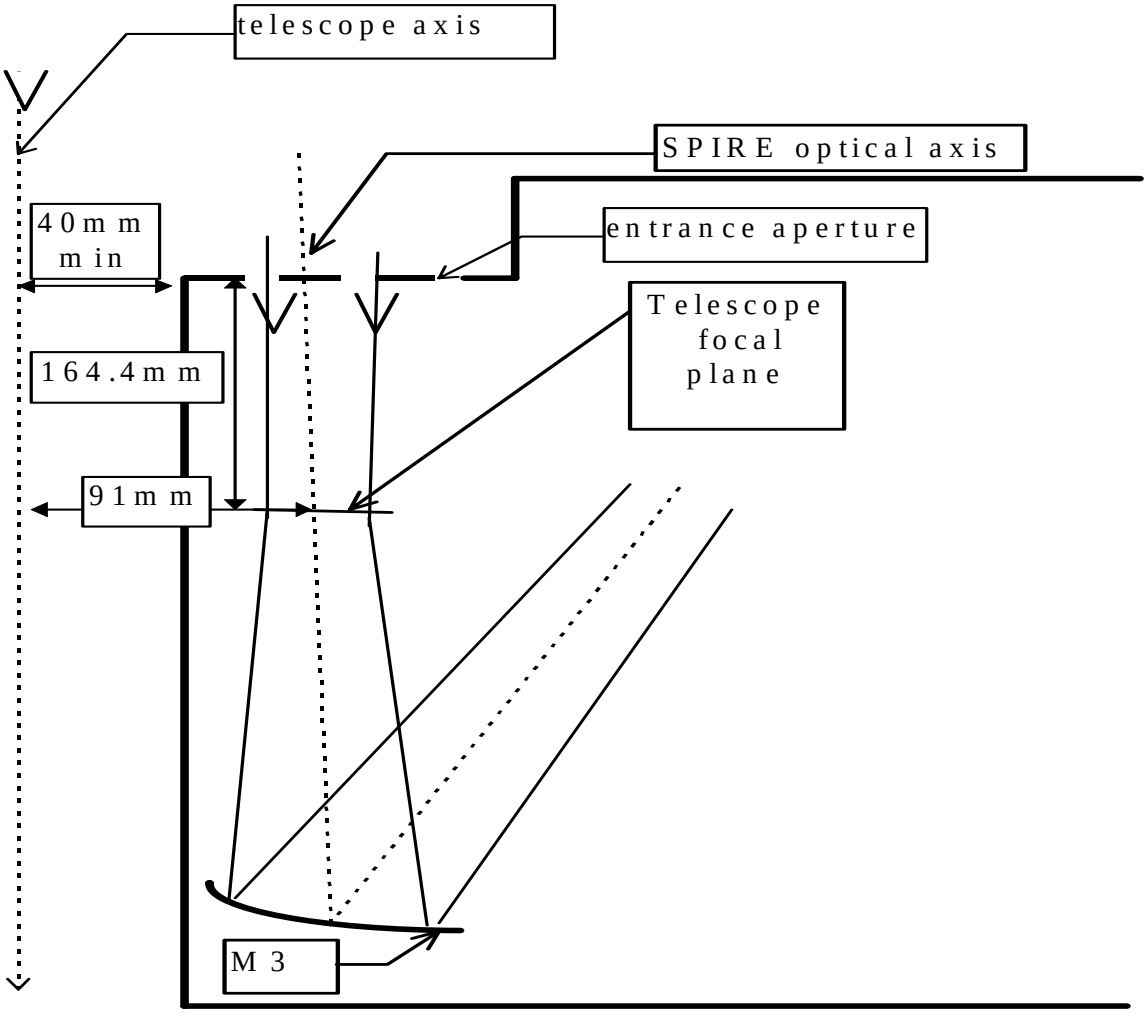

Figure 14 Clearance demanded between SPIRE enclosure and telescope axis

4.4.1 SPIRE entrance aperture

In the latest version of the CODEV model the SPIRE instrument enclosure's front aperture is surface 15. Figure 15 shows the footprint of the chopped detector view at this surface, together with a superimposed rectangle which has at least 6 mm clearance around the beam implied by the footprint. The rectangle has been taken as the template for an aperture to be located at the place shown in the SPIRE layout in figure 14 and a dummy optical surface with these dimensions has been added to the APART model of the instrument.

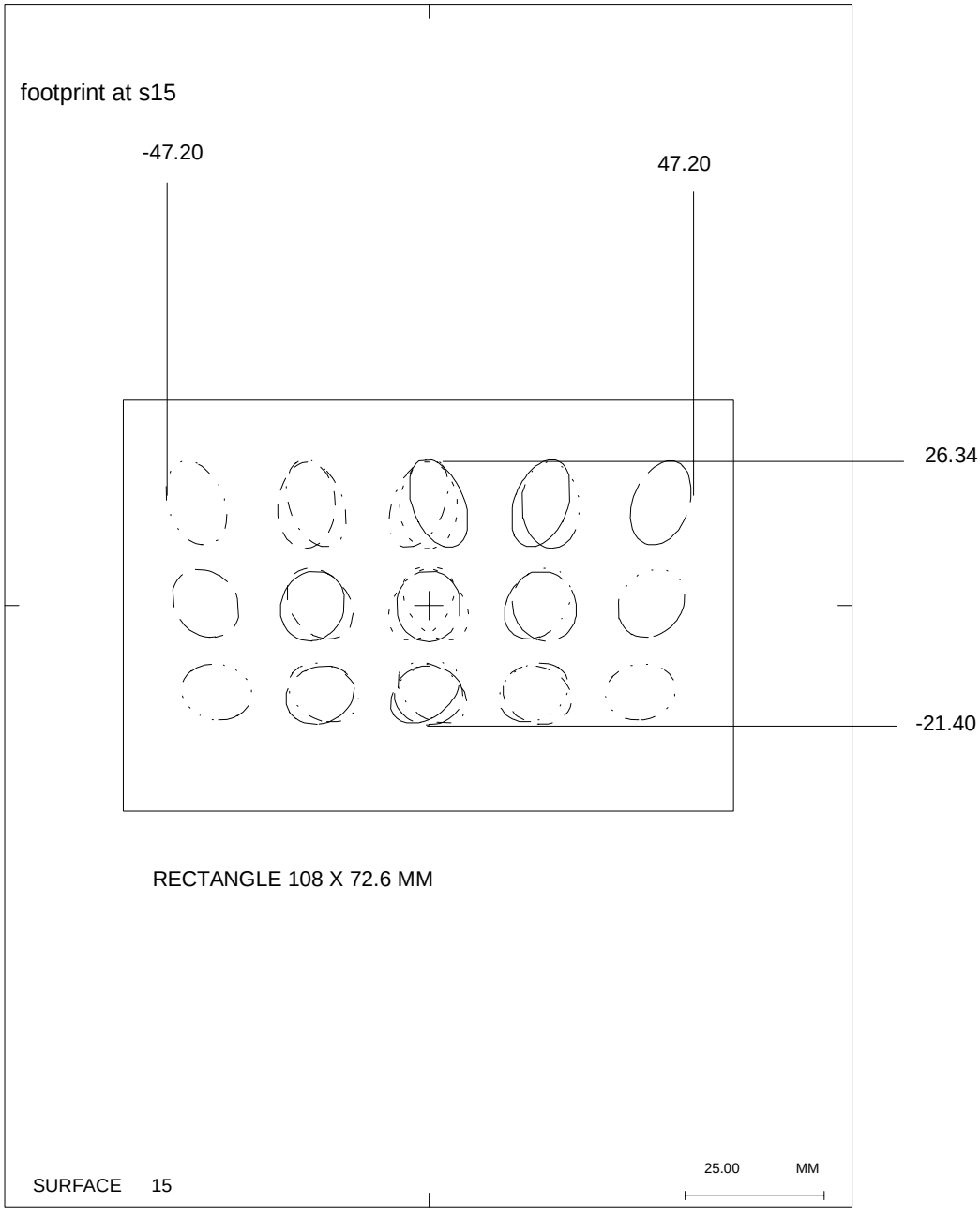

Figure 15 Composite beam footprint at location of proposed SPIRE instrument aperture

4.4.2 M3 mirror

The footprint at the first SPIRE mirror, usually labelled as M3 (M1 and M2 being respectively the FIRST primary and secondary mirrors) is shown in figure 16 accompanied by a rectangle which encloses the boundary of the M3 mirror proposed in the earliest references.

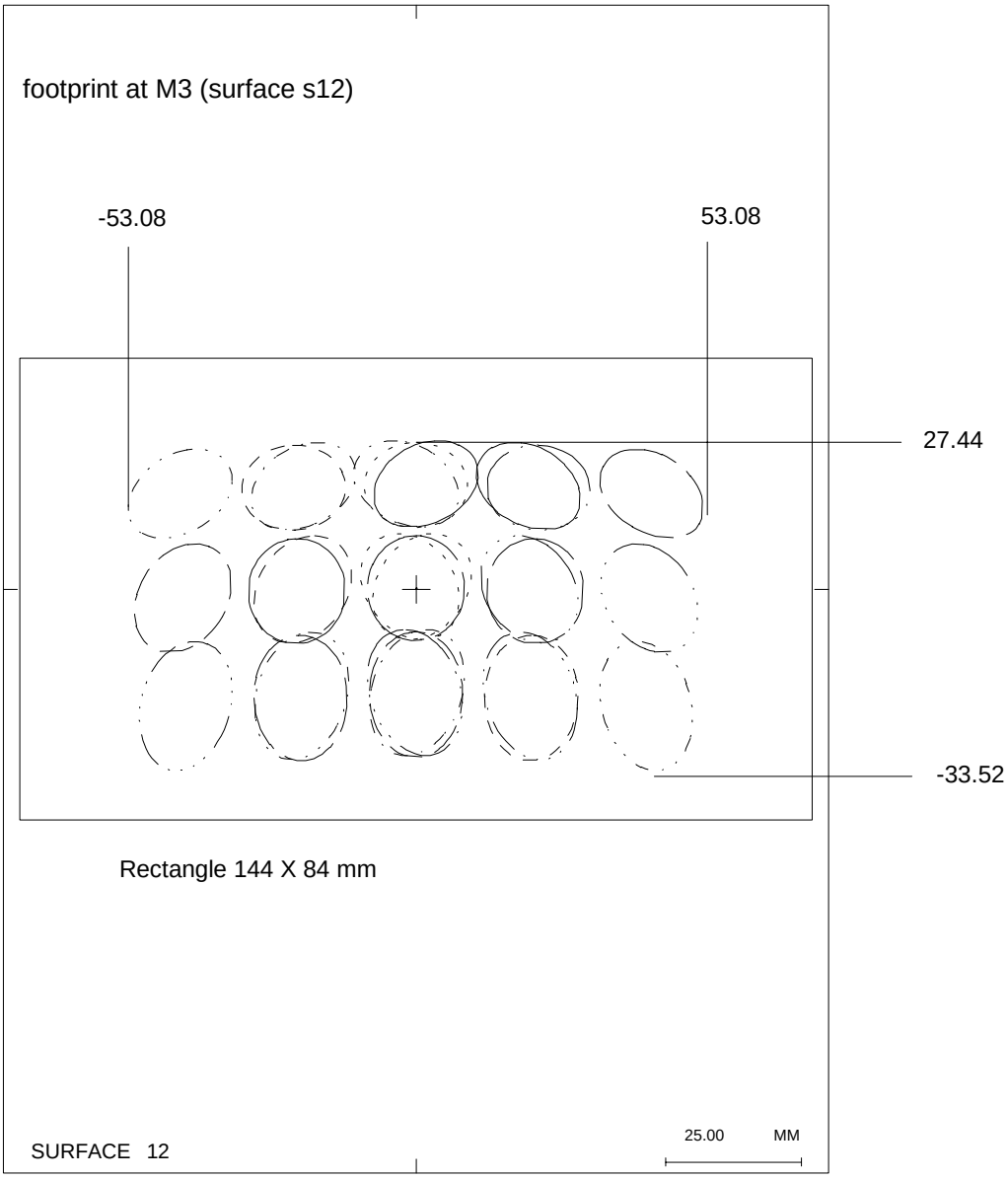

Figure 16 Composite beam footprint at location of M3

4.4.3 '4K filter'

The so-called '4K filter' is shown in figure 6 located between M3 and the chopper mirror, M4. Its location is actually 128.77 mm from M3 along the principal ray for the centre of the SPIRE FOV. The composite beam footprint at its location is displayed in figure 17 along with a rectangular aperture, offset towards -Y from the central principal ray, which will clear the footprint with at least 2.5 mm to spare.

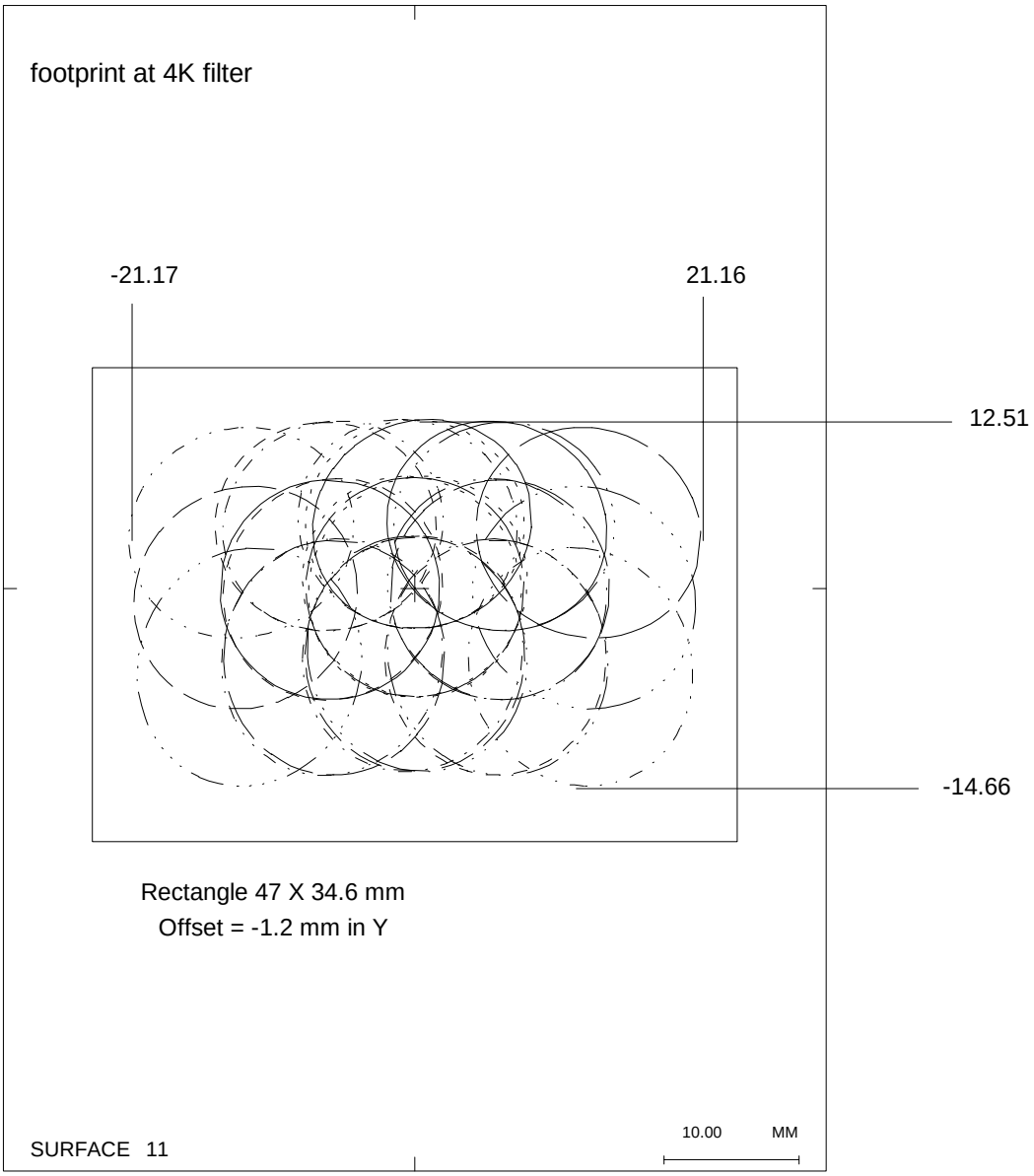

Figure 17 Composite beam footprint at location of '4K' filter

4.4.4 Chopper mirror, M4

Its location is 180 mm from M3 along the principal ray for the centre of the SPIRE FOV. The composite beam footprint at its location is displayed in figure 18 along with a 12 mm radius circular boundary, centred on the principal ray from the centre of the FOV, which will clear the footprint by at least 2.1 mm. The positions of the detector FOV footprint for each of the three chopper angles used (-3.964, 0, +3.964 deg.) can clearly be seen.

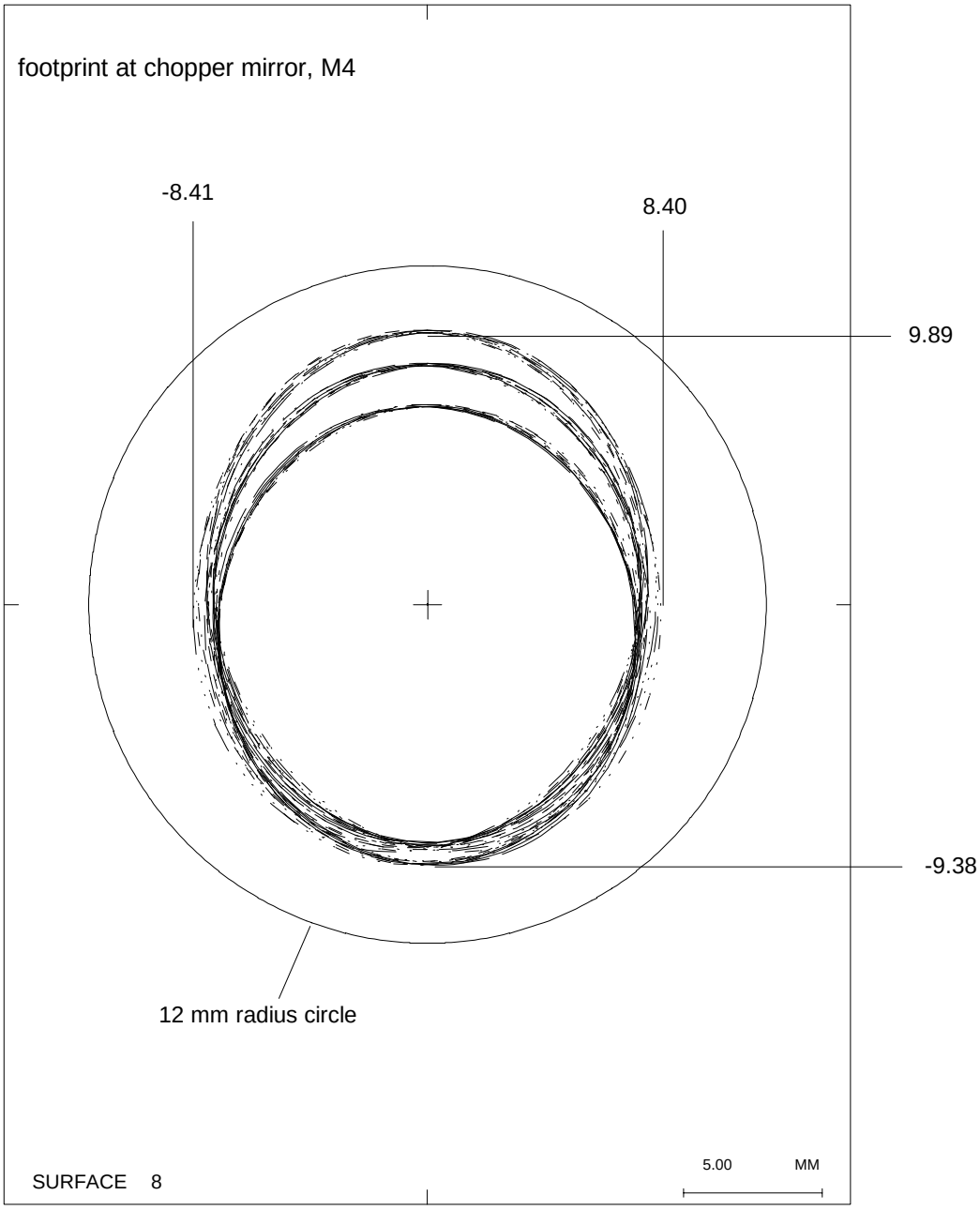

Figure 18 Composite beam footprint at chopper mirror, M4

4.4.5 Toroidal mirror, M5

Its location is 128.83 mm from M4 along the principal ray for the centre of the SPIRE FOV. The composite beam footprint at its location is displayed in figure 19 along with a rectangular boundary, centred on the principal ray from the centre of the FOV, which will clear the footprint by at least 3.7 mm. Because this component comes before the chopper mirror, there is no spreading of the footprint due to the chopper movement.

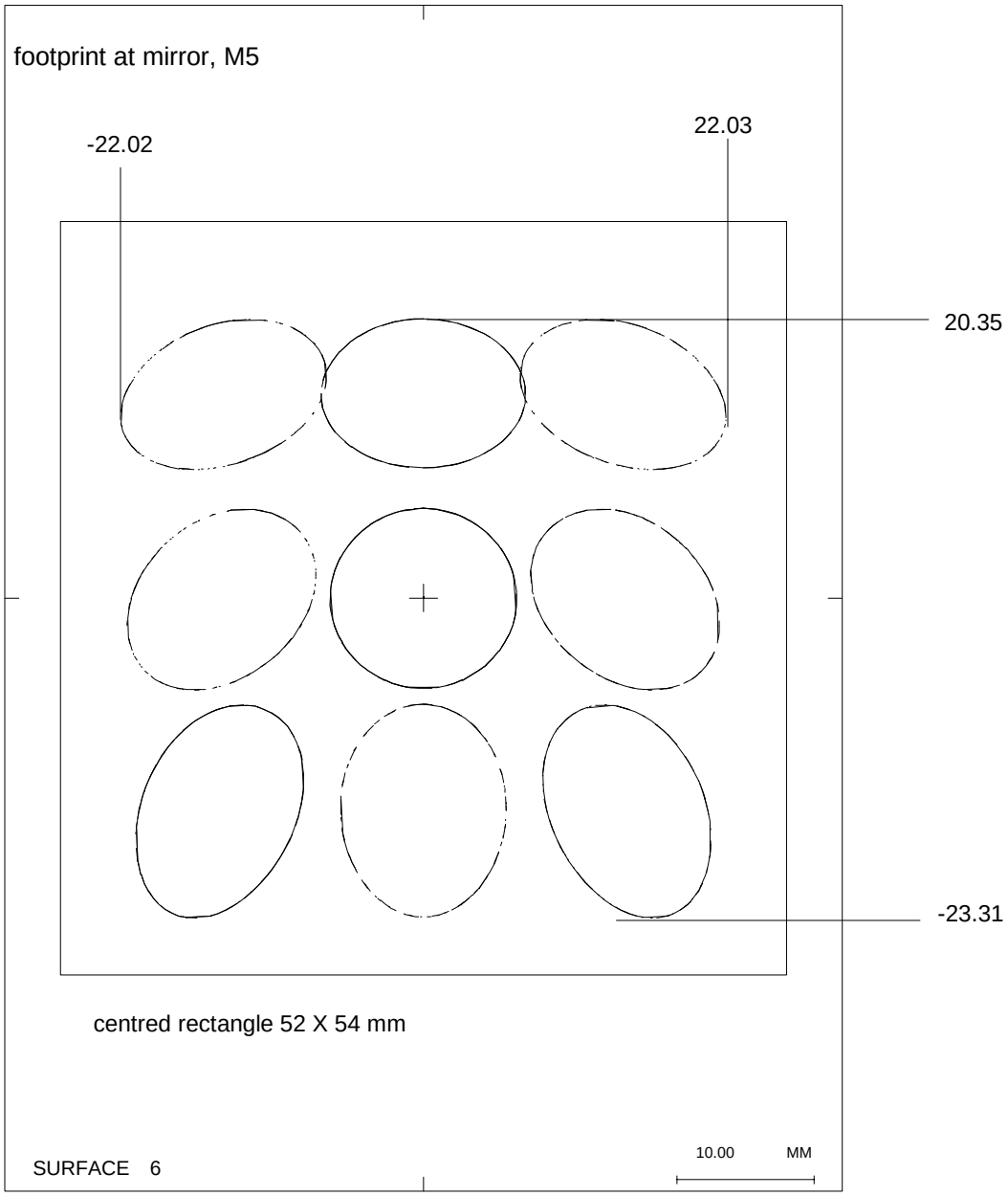

Figure 19 Composite beam footprint at mirror, M5

4.4.6 '2K filter' - re-imaged focal plane

The telescope focal plane is re-imaged at a position 84.467 mm from M5 along the principal ray for the centre of the SPIRE FOV. This is the location chosen for a '2K filter' which will be a window from the 4K-box into the so-called '2K-box'. The composite beam footprint at this location is displayed in figure 20 along with a rectangular boundary, centred on the principal ray from the centre of the FOV, which will clear the footprint by at least 1.5 mm. Because this aperture comes before the chopper mirror, there is no spreading of the footprint due to the chopper movement.

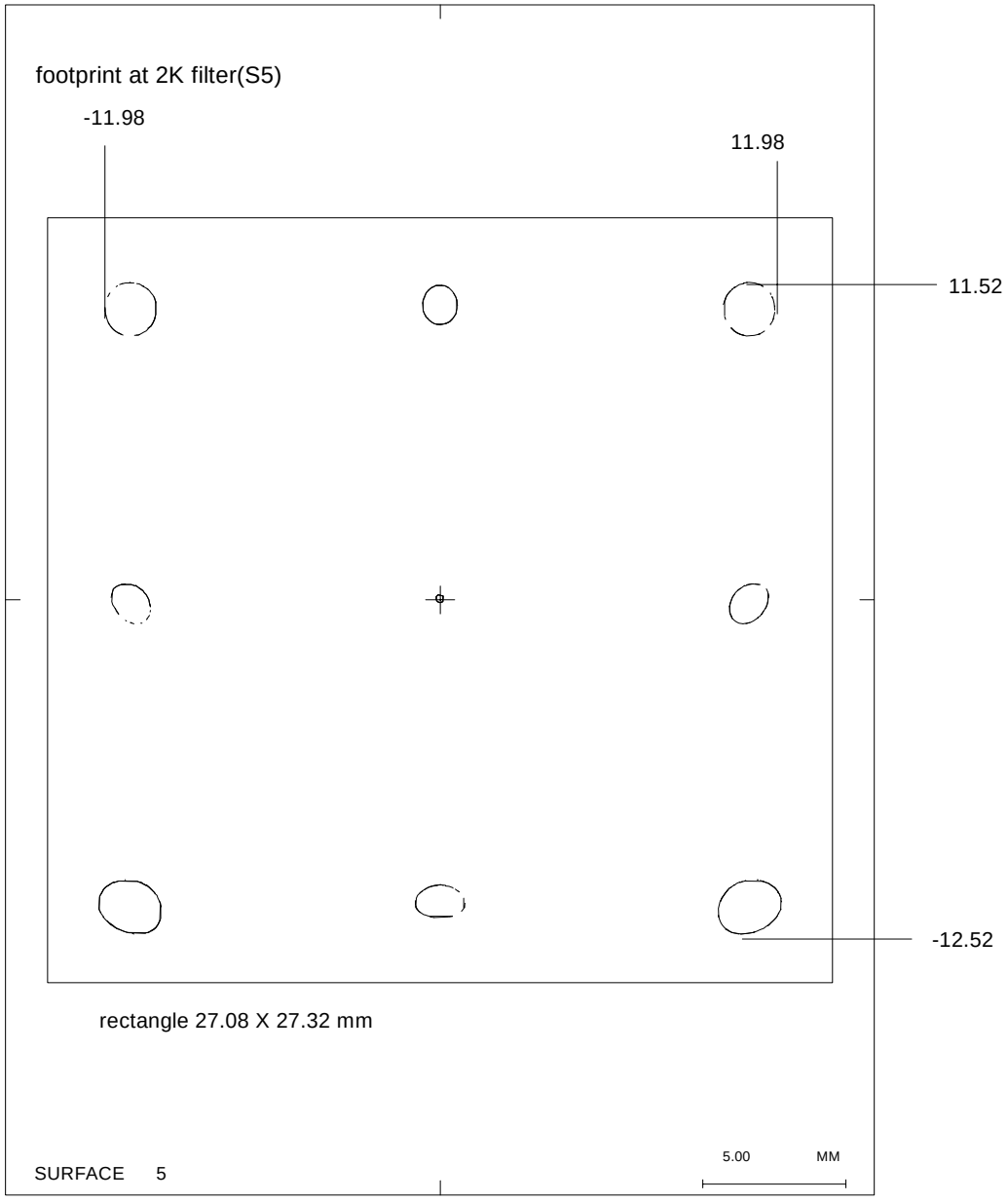

Figure 20 Composite beam footprint at '2K' filter location

4.4.7 Flat mirror, M6

M6 is 129.18322 mm from the '2K filter' located at the re-imaged focal plane, measured along the principal ray for the centre of the SPIRE FOV. The composite beam footprint at M6 is displayed in figure 21 along with a rectangular boundary, centred on the principal ray from the centre of the FOV, which will clear the footprint by at least 3 mm. Because this component also comes before the chopper mirror, there is no spreading of the footprint due to the chopper movement.

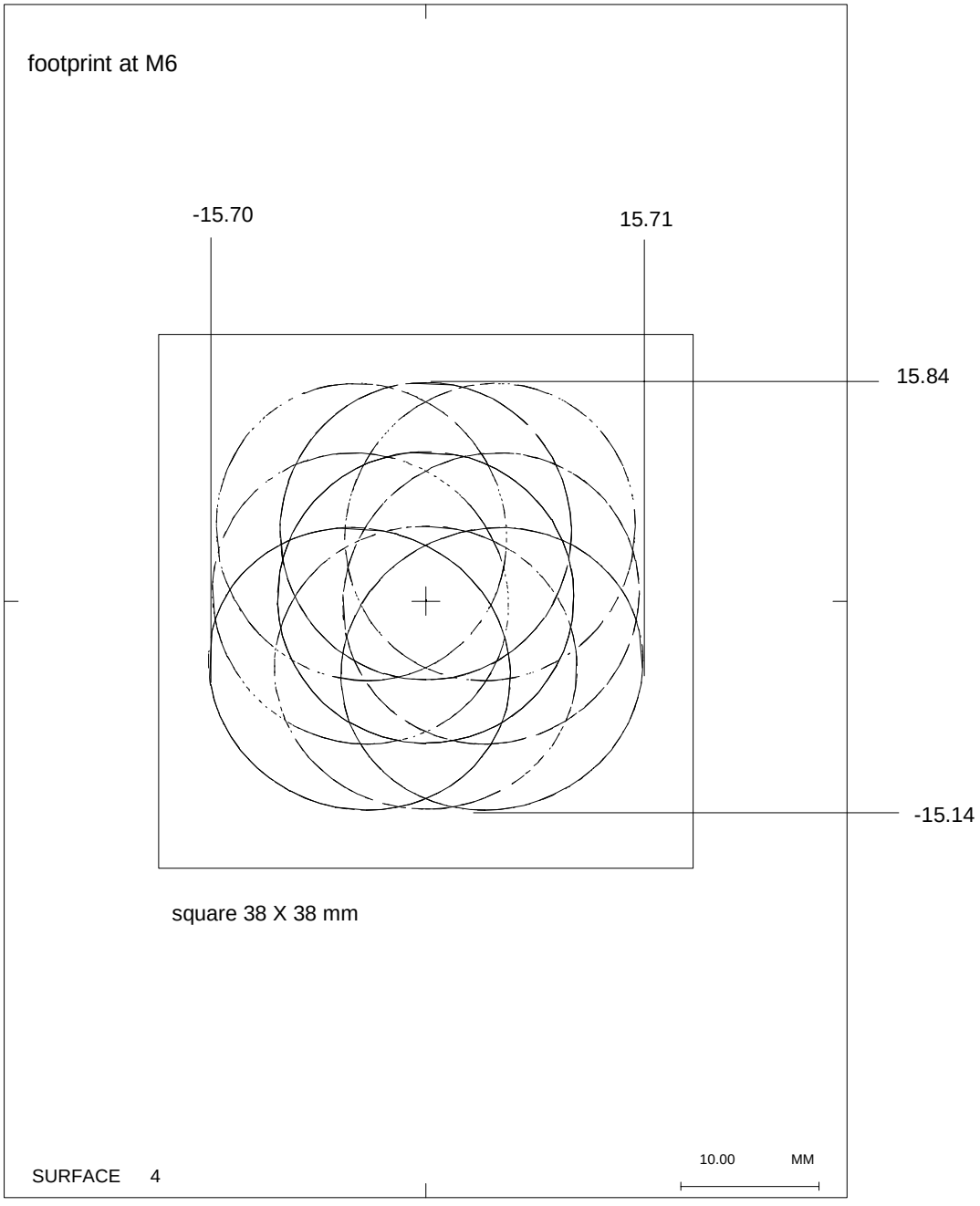

Figure 21 Composite beam footprint at flat mirror M6

4.4.8 Cold Stop

The cold stop is 100.34 mm from M6, measured along the principal ray for the centre of the SPIRE FOV. The composite beam footprint at the cold stop is displayed in figure 22. Since by definition all beams converge at the system aperture stop, the footprint is just the outline of the cold stop aperture.

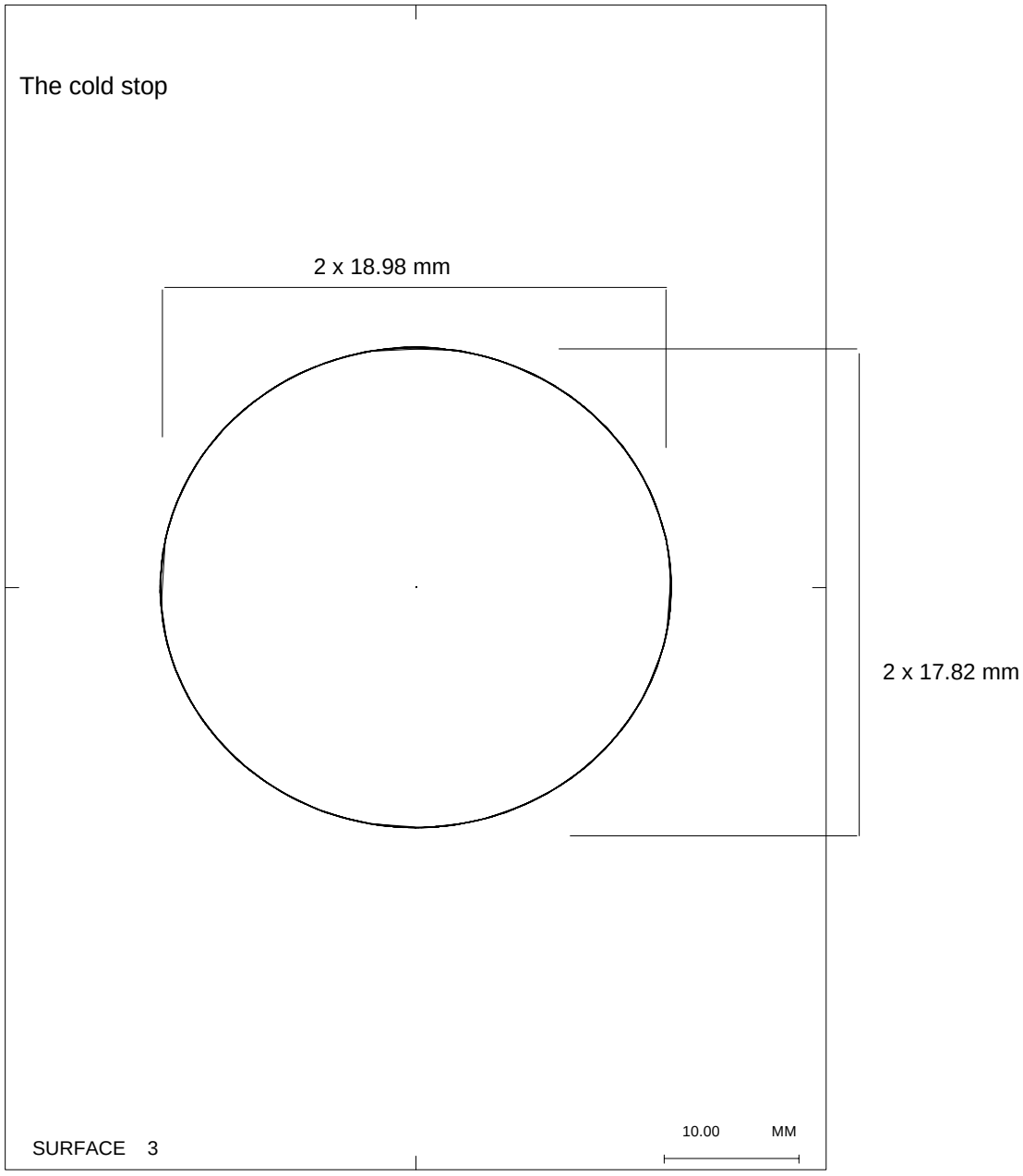

Figure 22 The beam footprint at the Cold stop

4.4.9 Toroidal mirror, M7

M7 is 150.0 mm from the cold stop, measured along the principal ray for the centre of the SPIRE FOV. The composite beam footprint at M7 is displayed in figure 23 along with a rectangular boundary, centred on the principal ray from the centre of the FOV, which will clear the footprint by at least 2 mm.

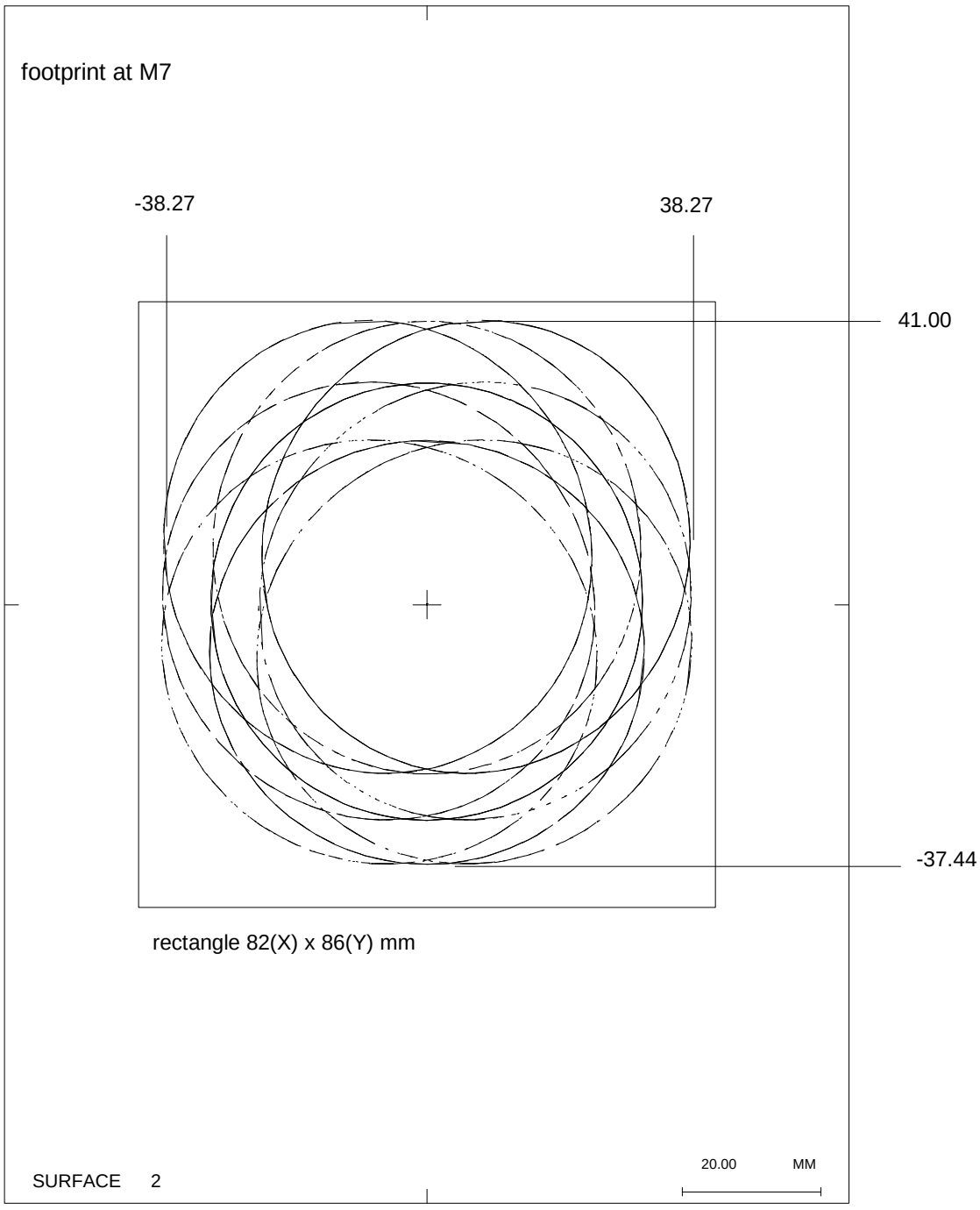

Figure 23 Composite beam footprint at toroidal mirror M7

4.4.10 Flat mirror, M8

M8 is 170.0 mm from M7, measured along the principal ray for the centre of the SPIRE FOV. The composite beam footprint at M8 is displayed in figure 24 along with a rectangular boundary, centred on the principal ray from the centre of the FOV, which will clear the footprint by at least 2 mm.

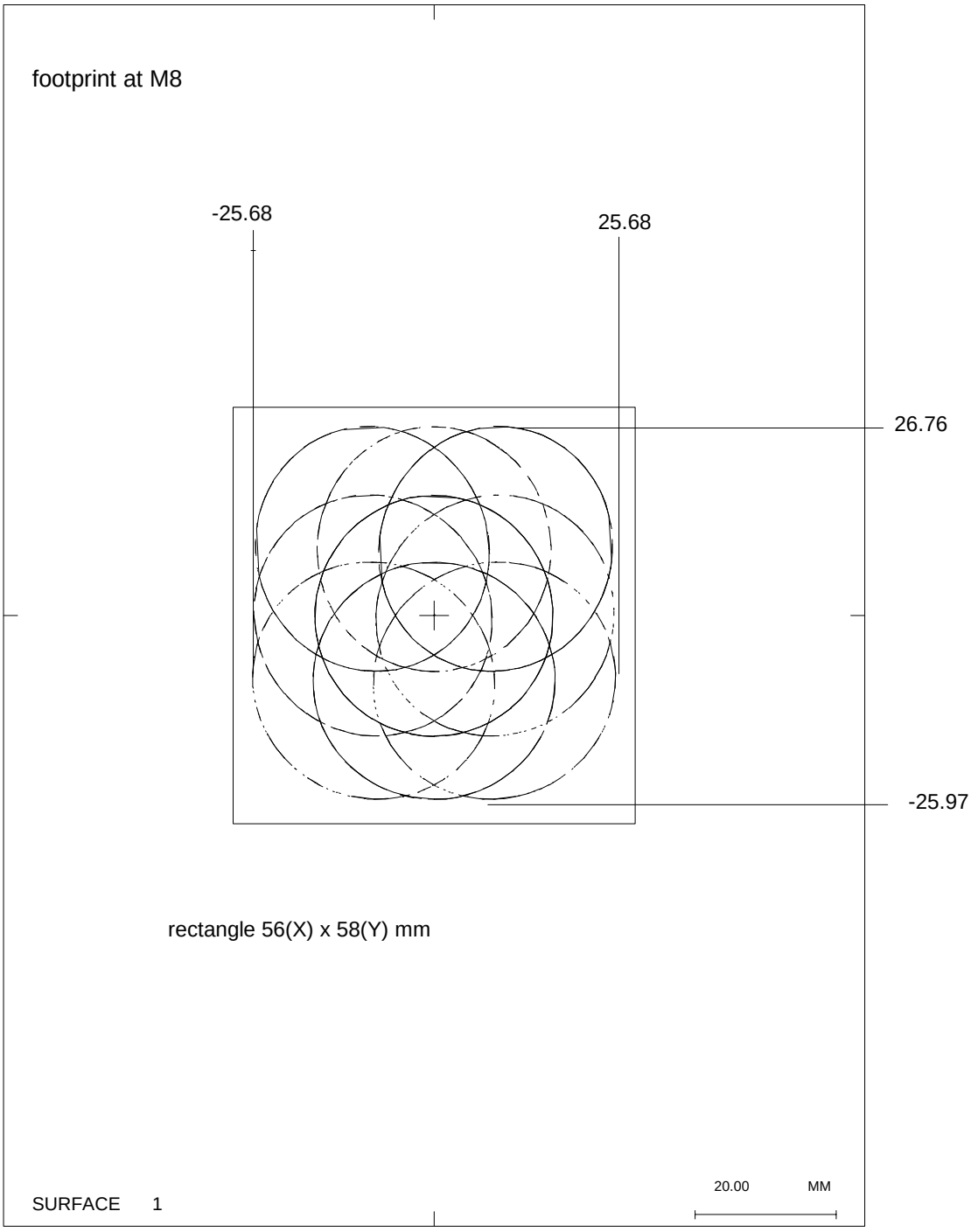

Figure 24 Composite beam footprint at flat mirror M8

5. CREATING AN APART MODEL FROM THE CODEV MODEL

An optical system which has been given a CODEV description can be converted into an APART version using the utility CDV2APRT.SEQ provided with the APART package. The CODEV system must be loaded and provided with the input direction of the 'gut ray' which will trace from the object space, through the system and finish up at the centre of the detector. This is done by inputting FIRSTBOL.SEQ at the CODEV command prompt. All that is then required is to input CDV2APRT.SEQ and the conversion process automatically takes place, the APART version of the system being listed to a file called FIRSTBOL.IN1.

There are a few limitations to the conversion process which are linked to the limitations of APART. Firstly, all non-optical surfaces in the CODEV model are not converted and are not replaced by APART versions in the output file. Thus if surfaces are wanted in the APART model at the locations of these non-optical surfaces, they will have to be added afterwards. Secondly, APART depends on paraxial imaging approximations and represents all curved optical surfaces as tilted spheres and so the conversion process will not necessarily produce optical surfaces with the exact curvatures and imaging properties of the CODEV optical surfaces. Warnings are produced in the APART listing of the system to this effect, although a system will be produced which correctly traces the gut ray so long as the latter traces through the CODEV system.

The accuracy of the conversion process can be checked by comparing data on the gut ray trace through the CODEV system (in particular angles of incidence and reflection from mirror surfaces) with the angular tilts applied to corresponding reflecting surfaces in the converted APART listing. To show this, table 5 gives the CODEV output resulting from tracing the gut ray from field point (XAN=0.0°,YAN=0.1829°) through the system.

The angles of incidence onto all the mirror surfaces must be reproduced as tilts in the APART converted file, which is displayed in table 6. Comparison of tables 5 and 6 shows that the conversion has been correctly done for the mirror surfaces. Note the warnings about the curvatures given to the original toroidal surfaces (M5 and M7) in the APART file. Note also the absence of the dummy CODEV surfaces. The distances along the gut ray between surfaces in the APART version can be compared with those listed in the CODEV gut ray-trace output in table 5 and shown to agree, so long as one sums the CODEV spacings with due regard to the changes in sign of the refractive index which take place at each mirror. Note that the spacings in the APART listing between optical surfaces are the sum of distances involving any intervening dummy surfaces, with each distance being given the sign of the refractive index in the space to which it applies. Thus the APART location for M4 is Z= 966.1882, which is the result of summing the spacings from primary M1 to M3 in the following way: -1396.922+0+0+1398.11+810.4789+164.5212+170-180, the changes of sign obeying the changes in sign of the refractive index at the secondary and M3. Armed with all the inter-surface distances given in table 5, one can subsequently add missing dummy surfaces to the APART model if desired.

Table 5 Angles of incidence and component spacings in the CODEV model

Surface	CODEV LABEL	ray intersept,mm (local co-ordinates)			ray angles on surface, degrees		surface spacing
description		X	Y	Z	incidence	reflection	along ray
object	OBJ	0	-3.19222E+07	0			
Primary,M1	1	0	-53.5989	-0.47154	1.19092	1.19092	-0.47154
Secondary,M2	STO	0	0	0	2.19894	2.19894	1396.922
dummy at M2	3	0	0	0	0	0	0
dummy at M2	4	0	0	0	0	0	0
dummy at primary hole	5	0	0	0	0	0	1398.11
dummy at front of SPIRE	6	0	0	0	0	0	810.4789
telescope focal plane	7	0	0	0	0	0	164.5212
dummy at M3	8	0	0	0	0	0	170
M3	9	0	0	0	14	14	0
dummy at M4	10	0	0	0	28	28	180
M4	11	0	0	0	28	28	0
dummy at M4	12	0	0	0	28	28	0
dummy after M4	13	0	0	0	0	0	0
M5	14	0	0	0	14	14	128.83
re-imaged focal plane	15	0	0	0	0	0	84.4666
M6	16	0	0	0	17	17	129.1832
cold stop	17	0	0	0	0	0	100.34
M7	18	0	0	0	22	22	150
M8	19	0	0	0	22	22	170
Detector	IMG	0	0	0	0		198

The curvatures given to all the curved surfaces in the APART file were checked against the radii of curvature given in the CODEV file and found to be correct, apart from those given for the toroidal mirrors, which differed slightly from the CODEV values, as expected.

6. MODIFYING AND DISPLAYING THE APART MODEL

The APART utility APMOD is the vehicle used for displaying the APART model and to verify the geometry of new surfaces which may be added to the model. Examples of the types of display possible are given in figures 25-28, which are four views of the initial APART model formed by converting the CODEV model. The plots show the optical surfaces in the SPIRE instrument, M3-M8, the re-imaged focal plane between M5 and M6, and also the system aperture stop between M6 and M7. None of the optical components or apertures have been given shapes or dimensions other than the default circular shapes allotted to them by APART using a tracing of the gut ray and a ray which traces to the edge of the detector through the edge of the aperture stop surface. The component sizing indicated from the study of the composite beam footprints was introduced to the model later and can be seen in figures 37-40.

Table 6 APART version of CODEV model

!**********CODEV to APART conversion**********	
! corrected BOL with ADE tilts for all optics	
!**	
* systems units are in millimeters	
* wavelength is 200.000000 microns	
DISK 1 6 -1 0.0000 1722.717 0.000 (MIRROR 1)	primary mirror M1 at Z=0
REFL	refractive index changed to -1
CV -0.00032827	curvature at pole
CC -1.000000	conic constant
DEC -53.5989	gut ray Y coord 53.5989
ROTATE X 1.1909	angle of incidence=1.1909
DISK 2 6 1 -1396.9219 140.000 0.000 (ASTOP 2)	Secondary,M2,spacing at Z=-1396.9219
REFL	refractive index changed to +1
CV -0.00373371	curvature at pole
CC -1.238772	conic constant
ASTOP	mark it as aperture stop
ROTATE X -2.1989	angle of incidence=2.1989
DISK 3 6 -1 -1396.9219 141.467 0.000 (OPTIC 3)	dummy optic at M2
OPTIC 1.000000 !	refractive index still =+1, no reflection
CV 0.00000000	flat
DISK 8 6 -1 1146.1883 34.802 0.000 (MIRROR 8)	M3
REFL	reflector, refractive index changed to -1
CV -0.00294118	curvature at pole
ROTATE X 14.0000	angle of incidence=14
DISK 10 6 1 966.1882 11.327 0.000 (MIRROR 10)	M4
REFL	reflector, refractive index changed to +1
CV 0.00000000	flat (curvature 0)
ROTATE X -28.0000	angle of incidence=28
DISK 13 6 -1 1095.0182 23.991 0.000 (MIRROR 13)	M5, toridal
REFL	reflector, refractive index changed to -1
CV -0.00510939	mean curvature where gut ray hits
!***THIS SURFACE IS PROBABLY NOT CORRECT***	caveat regarding inaccurate portrayal of non-spherical surfaces
ROTATE X 14.0000	angle of incidence=14
DISK 15 6 1 881.3684 20.362 0.000 (MIRROR 15)	M6
REFL	reflector, refractive index changed to +1
CV 0.00000000	flat (curvature 0)
ROTATE X -17.0000	angle of incidence=17
DISK 17 6 -1 1131.7084 45.887 0.000 (MIRROR 17)	M7, toroidal
REFL	reflector, refractive index changed to -1
CV -0.00247685	mean curvature where gut ray hits
!***THIS SURFACE IS PROBABLY NOT CORRECT***	caveat regarding inaccurate portrayal of non-spherical surfaces
ROTATE X 22.0000	angle of incidence=22
DISK 18 6 1 961.7084 30.011 0.000 (MIRROR 18)	M8
REFL	reflector, refractive index changed to +1
CV 0.00000000	flat (curvature 0)
ROTATE X -22.0000	
DISK 19 6 -1 1159.7084 55.095 0.000 (IMAGE 19)	Detector
CV 0.00000000	

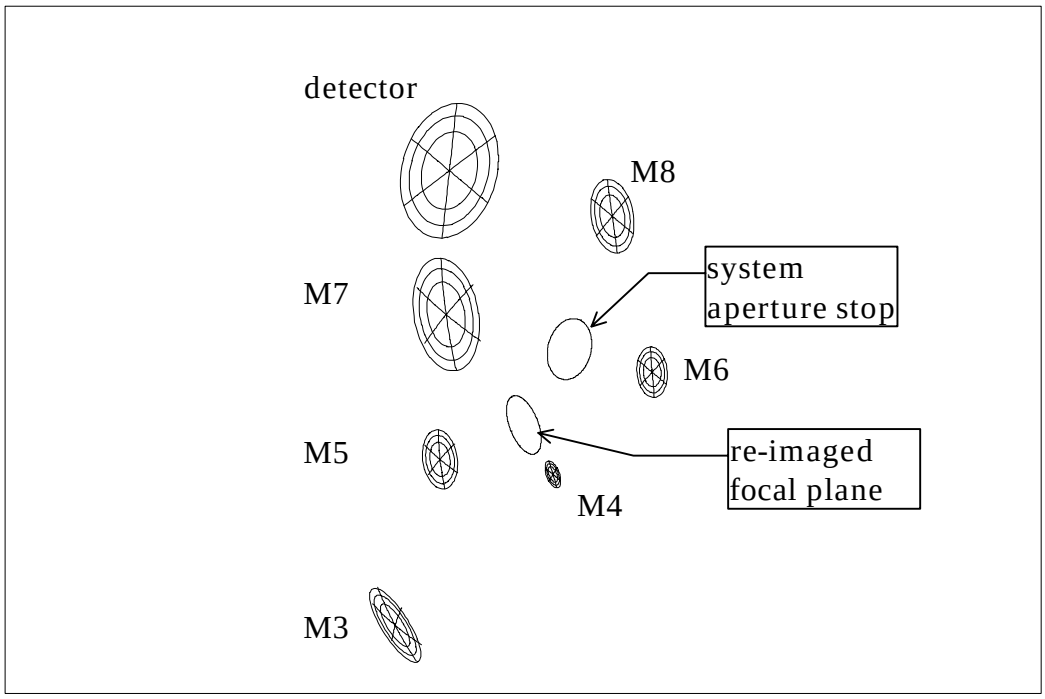

Figure 25 3D view, output by APMOD, of the APART model of the SPIRE optics

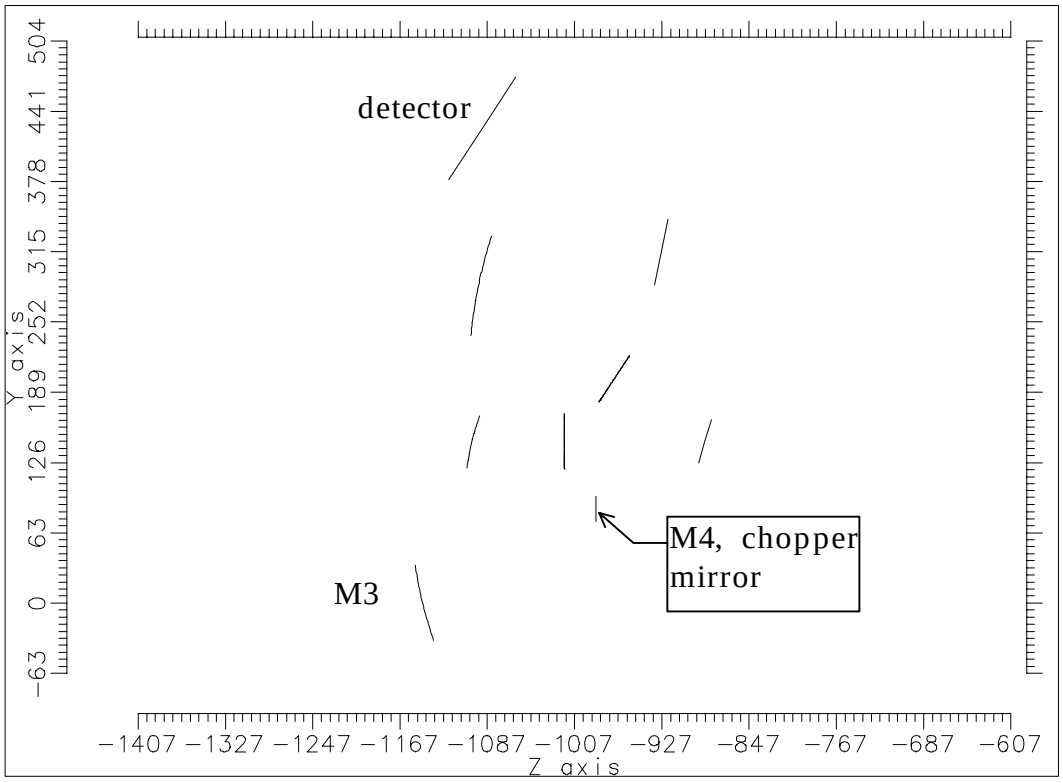

Figure 26 YZ-view of converted APART model of the SPIRE optics

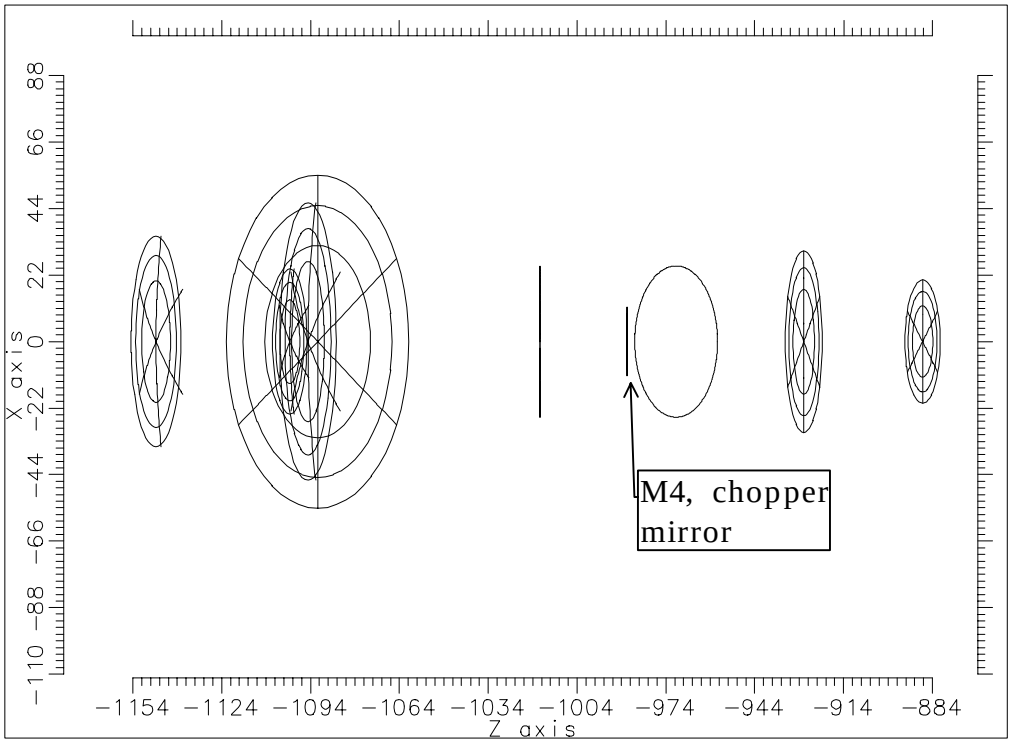

Figure 27 ZX-view of APART model of SPIRE optics

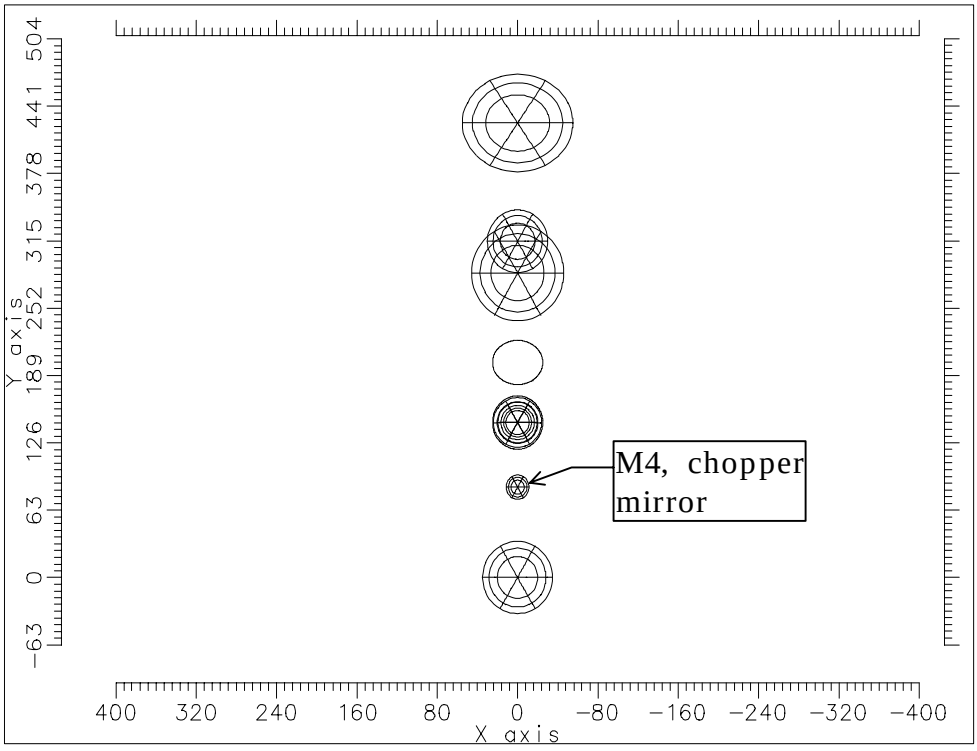

Figure 28 XY-view of APART model of SPIRE optics

The plots in figures 25-28 illustrate the general co-ordinate orientation of the system, with the SPIRE optics spread out parallel to the telescope's Y-Z plane in the +Y direction. The rotation of the chopper mirror, M4, is such as to tilt the beam out of the Y-Z plane, its axis of rotation being parallel to the Y direction in figures 26 and 28.

7. ADDING STRUCTURE TO THE APART MODEL

The APART model requires the addition of various structures in order to be considered a realistic model of the FIRST-SPIRE system. Principal among these are

- Surfaces representing the outer edge of the secondary mirror, the inside of the hole in the primary mirror and the rear of the primary visible through the cryostat aperture. Secondary mirror support strut surfaces which face the primary and secondary..
- Surfaces inside the cryostat chamber visible from the entrance aperture of SPIRE
- Surfaces surrounding SPIRE optics up to and including the 2K filter location

Because the emission from surfaces at 2K and below can be neglected, it is only necessary to include optical surfaces (including the cold stop) in that part of the SPIRE instrument from the 2K aperture to the detector.

7.1 Telescope surfaces

These consist of a conical surface acting as the edge of the secondary and flat surfaces representing those parts of three equispaced struts (at 12 o'clock, 8 o'clock and 4 o'clock) which face the primary mirror and extend from the edge of the secondary to the edge of the primary. Also added are a 130 mm radius cylindrical surface representing the wall of the hole in the primary, a 130 mm radius flat surface representing the hole opening and a plane annular surface representing that area behind the primary outside the hole which can be viewed from within the SPIRE instrument through the SPIRE optics and through the cryostat apertures. Plots of these surfaces are provided in the following figures.

7.2 Cryostat surfaces

The cryostat is at present modelled as two cylinders co-axial with the telescope axis and two annular surfaces at 90 degrees and concentric with the telescope axis. The inner radii of the annular surfaces and the radius of the smaller cylinder is set = 130 mm. These surfaces are displayed in accompanying plots. Also shown in figure 35 is an extra hemispherical surface with a central hole which has since been added to represent all surfaces which occupy the solid angle outside that occupied by the rear aperture of the rear part of the cryostat tube, nearest to SPIRE, when viewed from a point at the centre of the SPIRE entrance aperture.

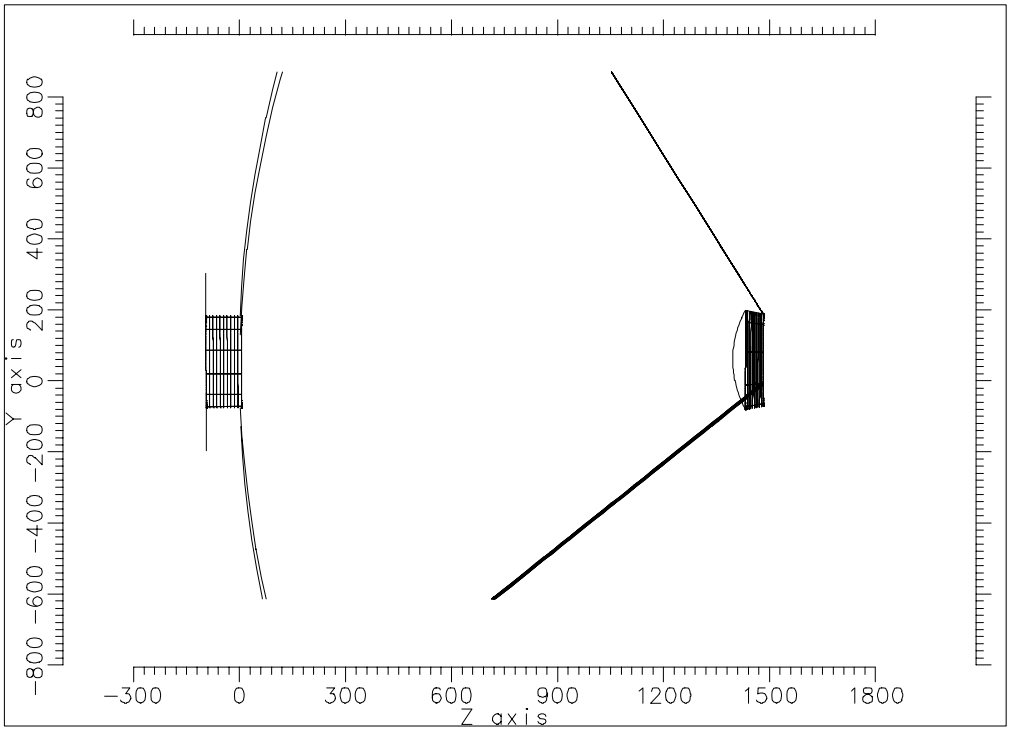

Figure 29 YZ-section plot of APART telescope surfaces (truncated)

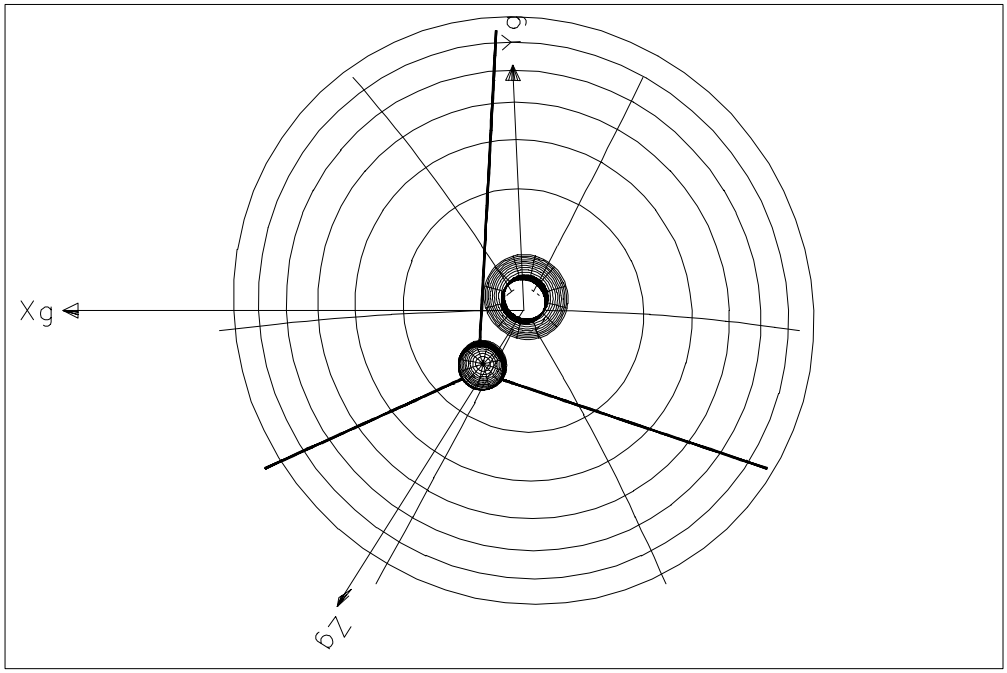

Figure 30 3D plot of APART telescope surfaces

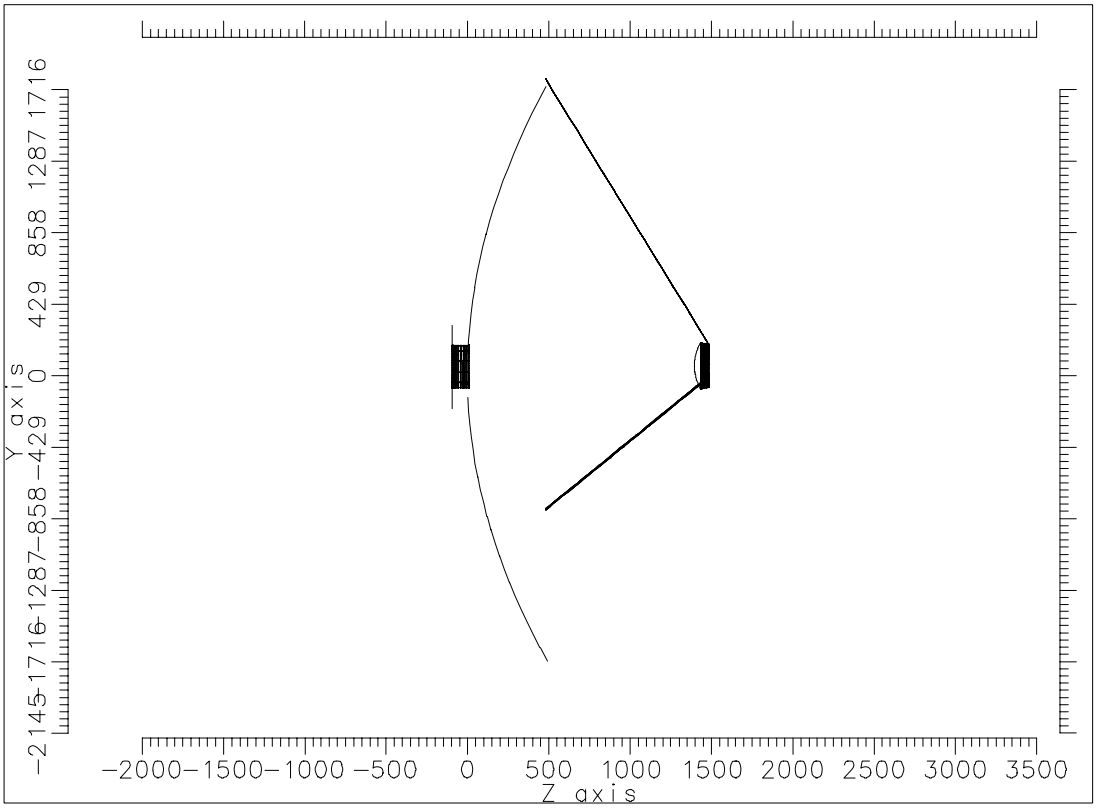

Figure 31 Full YZ-section plot of APART telescope surfaces

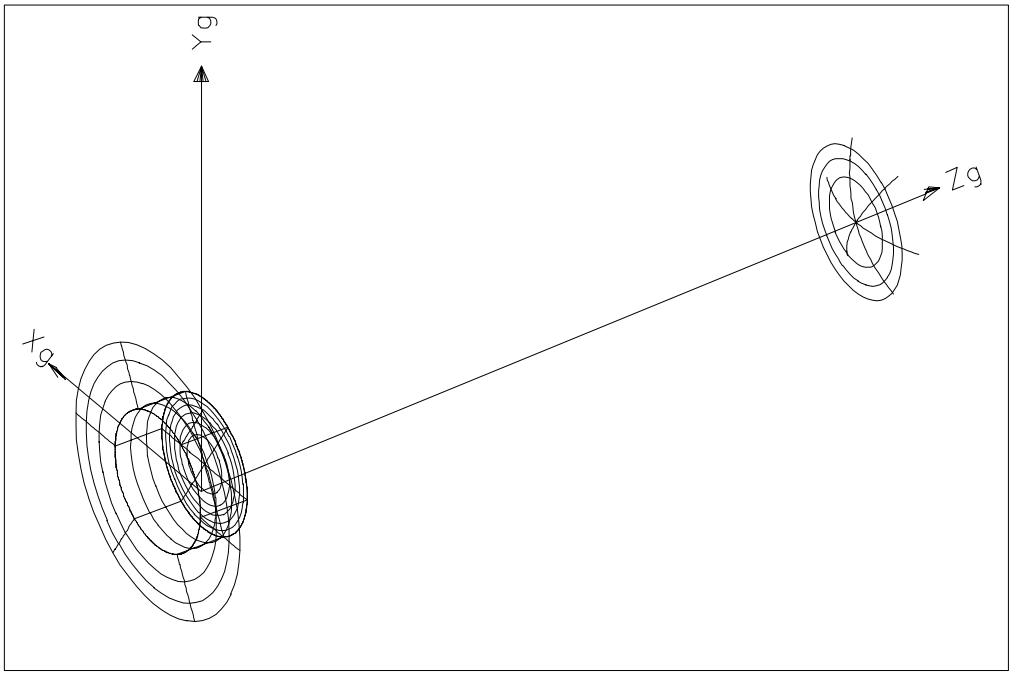

Figure 32 View of primary hole surfaces and secondary mirror surface

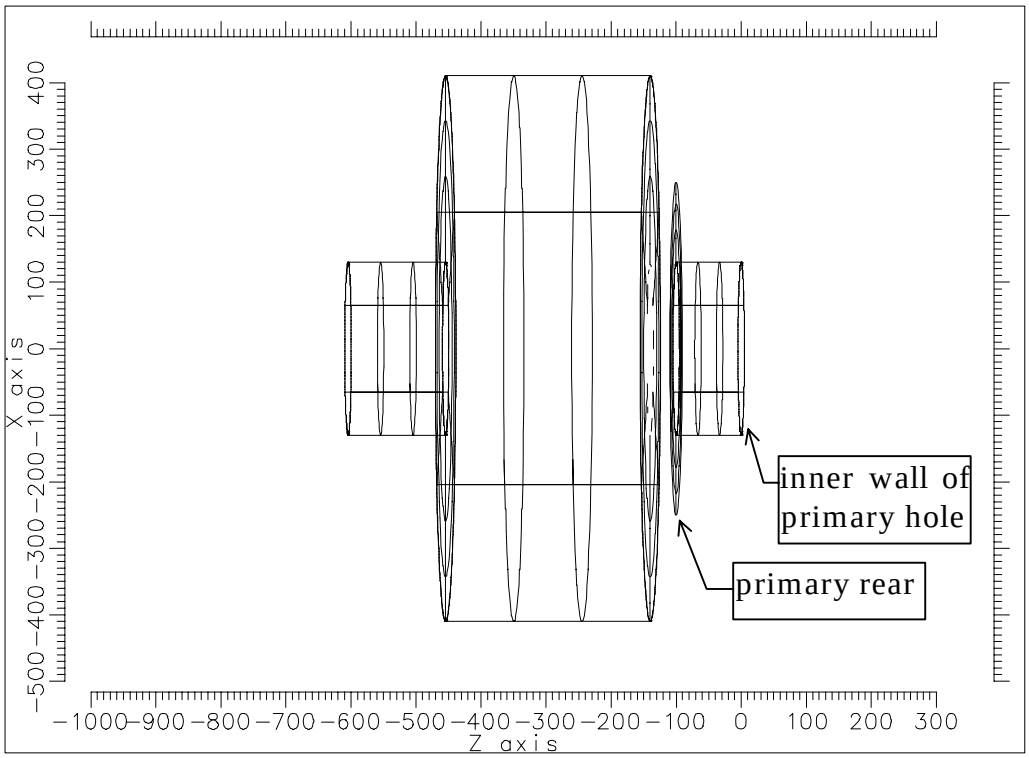

Figure 33 XZ-section plot of APART cryostat surfaces+primary hole and rear

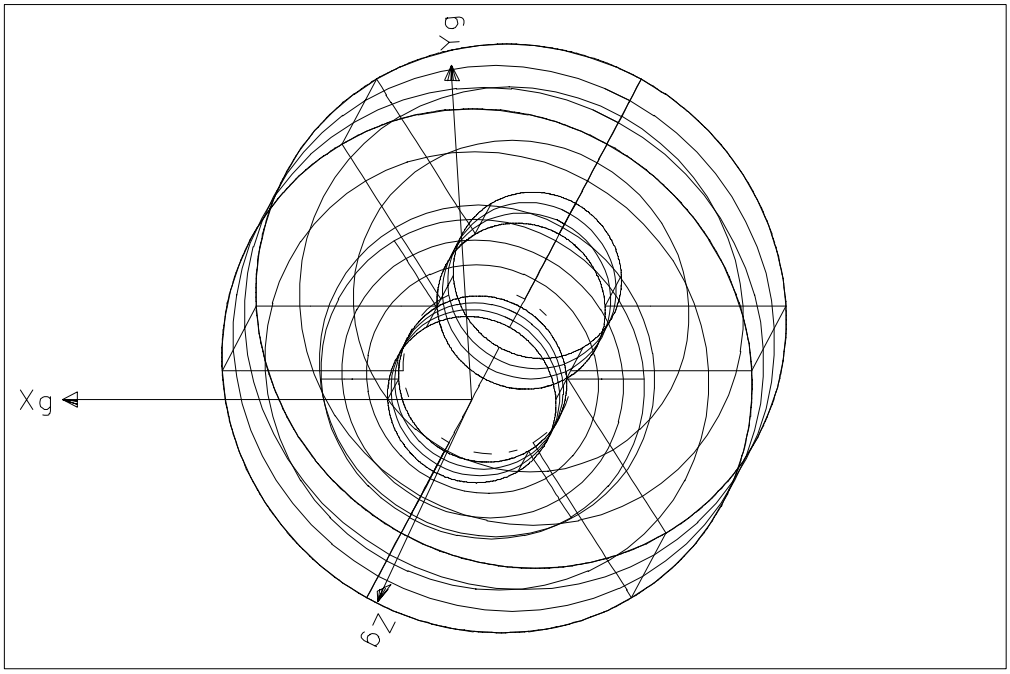

Figure 34 3D plot of APART cryostat surfaces+primary hole and rear

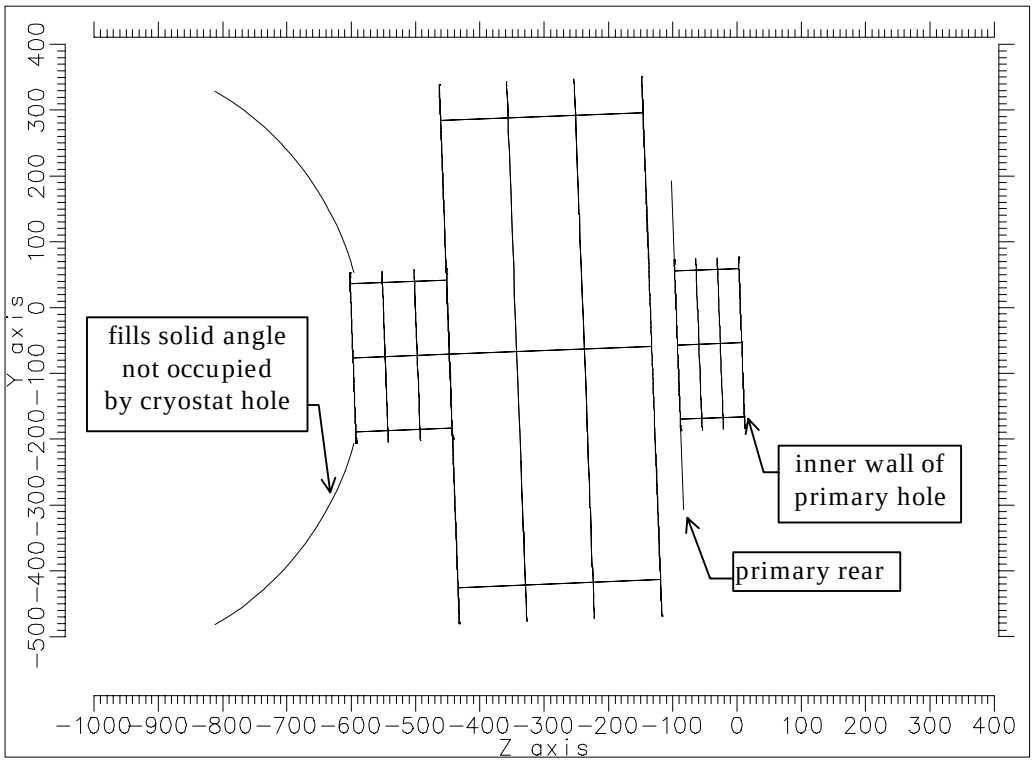

Figure 35 YZ-section plot of APART cryostat surfaces + surface representing all surfaces outside cryostat rear aperture

7.3 SPIRE structural surfaces

Figure 36 indicates the locations presently selected for boundaries of surfaces which are to represent SPIRE structure. The plane of the drawing is parallel to the telescope Y-Z plane. Surfaces labelled 'S' are 'side' surfaces oriented parallel to the telescope X-Z plane. A surface labelled 'T' and 'B' represents identically-shaped 'top' and 'bottom' surfaces which are located at X=+80mm and X=-80mm above and below the telescope Y-Z plane and oriented parallel to the Y-Z plane. The value 80 mm for all such surfaces is based on the need to clear the largest optic and the arbitrary assumption that they can be co-planar. The details of the geometry of each surface were essentially fixed using a scaled drawing of the SPIRE optical layout and figure 6 as a guide to where there are likely to be structural and filter surfaces, the philosophy being to place easily-modelled surfaces either at the expected location of structural surfaces or close enough to them so that the model surfaces occupy the same solid angle as real structure when viewed from important apertures and optics. Figures 37-40 show plots of those parts of the APART model which have been created from these model surfaces. Accompanying the added structural surfaces are the SPIRE optical surfaces as they are now represented in APART. In some cases, a rectangular boundary which was drawn around a beam footprint on an optical component (see earlier figures showing CODEV-traced footprints) has been modified to have rounded corners.

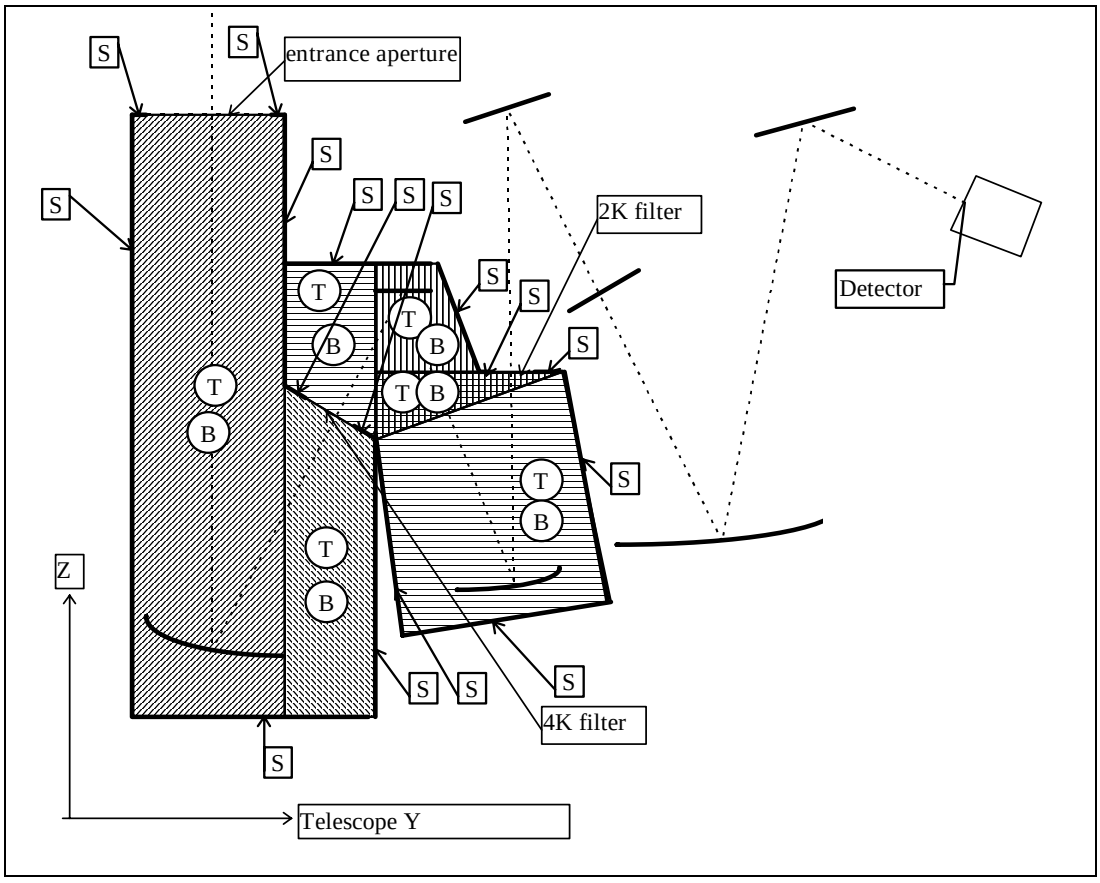

Figure 36 Schematic outlines of SPIRE structural surfaces which have been added to the APART model

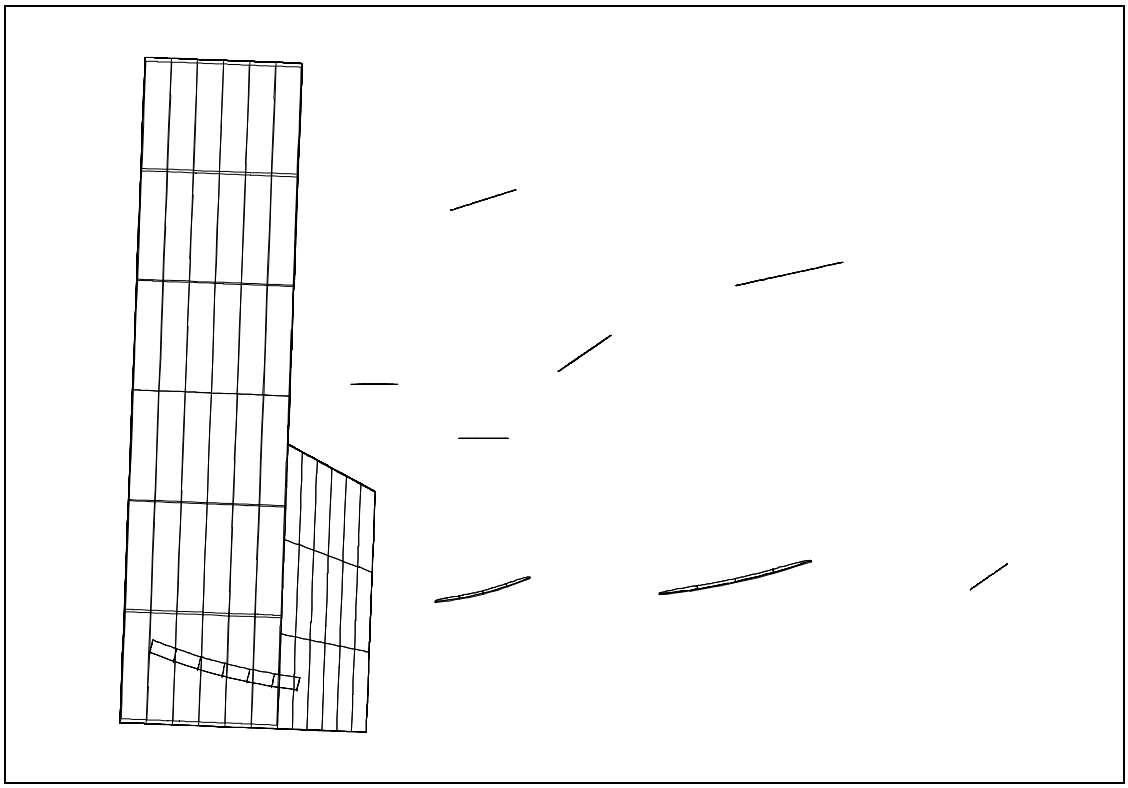

Figure 37 Y-Z plot of '15K' structure added to APART model

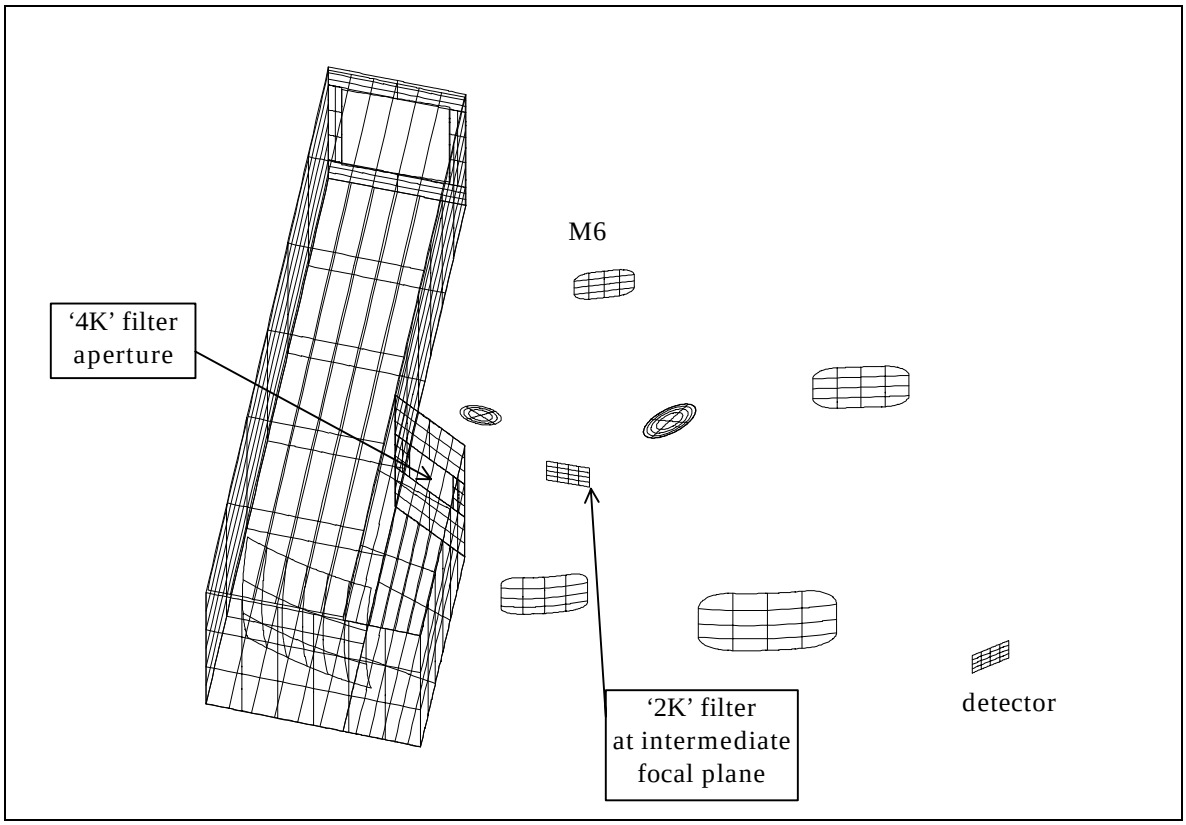

Figure 38 Isometric plot of '15K' structure showing relationship to optical surfaces

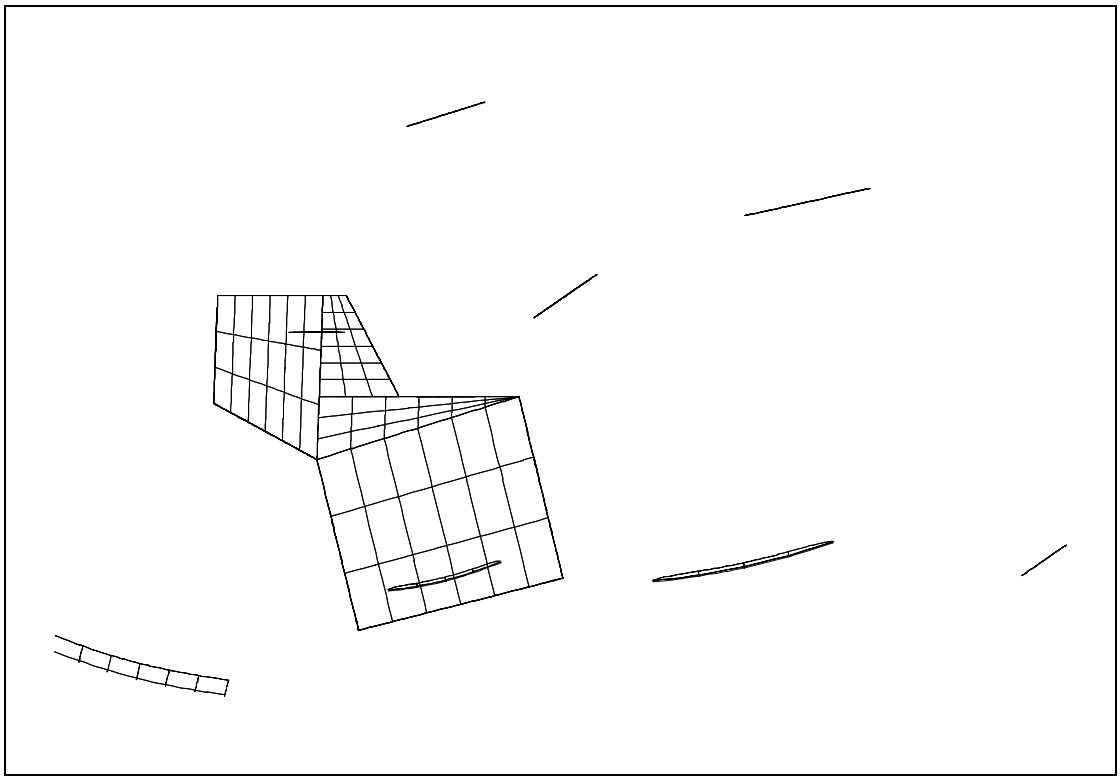

Figure 39 Y-Z plot of '4K' structure added to APART model

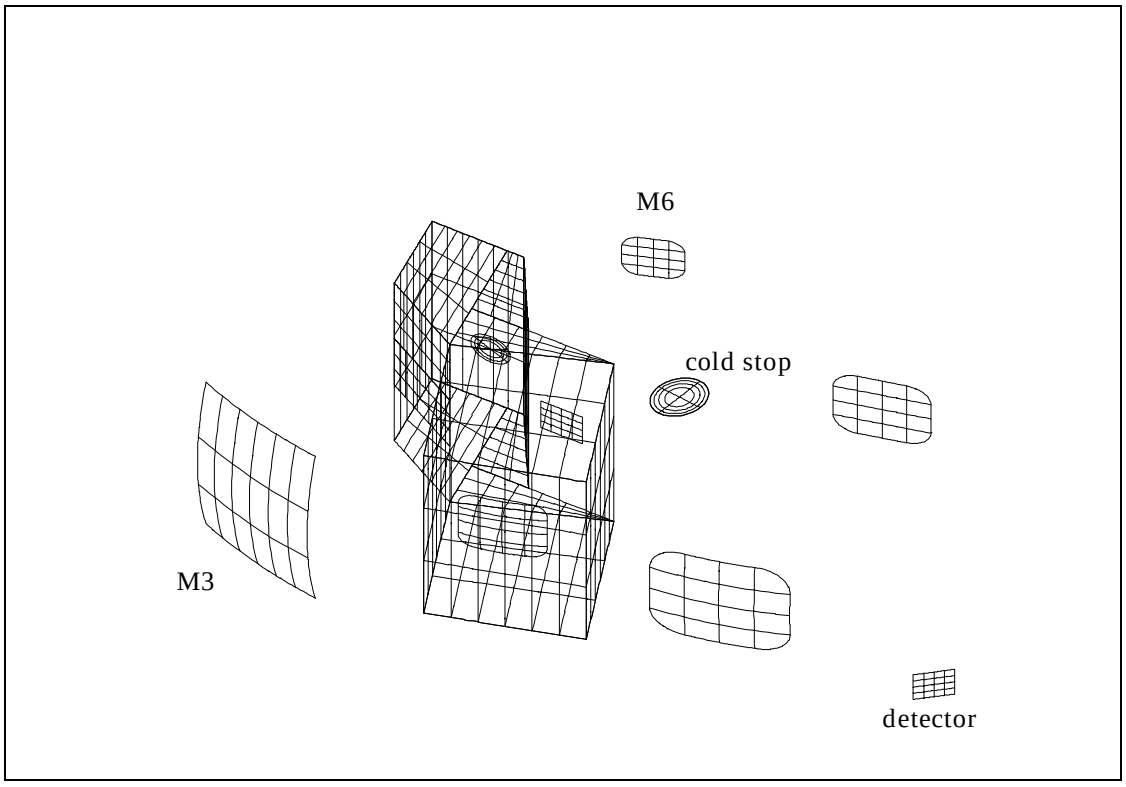

Figure 40 Isometric plot of '4K' structure showing its relationship to optical surfaces

8. IGES INTERFACE

All of the figures displaying APART structure have been created from ASCII files of type .HPG which contain Hewlett Packard Graphics Language(HGL) commands. As well as these files, plot files of type .VC1 which contain simple 3-D vector plot commands can be simultaneously produced by APMOD and there exists a graphics filter which can process these latter .VC1 files into an IGES-formatted file containing simple line entities. This filter was written as part of the GERB project and it has been shown to produce IGES-formatted output which can be successfully ported to the Pro-Engineer CAD platform. Thus it should be possible to merge and compare APART structural geometry with any other SPIRE structure which may be defined using a CAD package which has a standard IGES import capability.

9. COMMENTS

It is hoped that the preceding notes have made clear how the uncertainties surrounding the FIRST telescope and cryostat design will impact on the SPIRE optical and straylight control design. It is important that SPIRE have early access to information coming out of the development of the telescope and cryostat designs so that the impact of these developments on the SPIRE instrument can be assessed and responded to.

Also it should be clear that the present SPIRE imaging performance has lead to a reduction in throughput because of the need to reduce the system aperture stop dimensions in order

to prevent the FOV being vignetted at the secondary mirror of the telescope, presently assumed to have a 130 mm radius. It follows that some effort needs to be put into determining where best improvements to the optical design can be made. This process will require the SPIRE consortium receiving up-to-date knowledge of the optical parameters defining the FIRST telescope mirrors and knowledge of any proposed changes in the relative position of the SPIRE FOV within the telescope's FOV.

10. APPENDIX: CODEV SEQUENCE FILES FOR THE SPIRE BOLOMETER

10.1 Sequence file FIRSTBOL.SEQ defining the system traced from space to detector

```
RDM;LEN      "VERSION: 8.11 A      LENS VERSION: 43      Creation Date: 27-JAN-1998"
TITLE 'corrected SPIRE with ADE tilts for all optics'
EPD   3335.03281138
DIM   M; WL    200000.0
REF   1; WTW   1;INI  ' '
CA    APE
XAN   0.0 0.04307
YAN   0.1829 0.1829
VUX   0.0 0.0;VLX   0.0 0.0;VUY   0.0 0.0;VLY   0.0 0.0
SO    0.0 0.1e11                    !object surface at infinity
S     -3046.246 -1396.3648 REFL     ! primary mirror
 CON;  K   -1.0
S     -267.82995 0.0 REFL           ! secondary mirror
 STO;  CON;  K   -1.2387718
 DAR;  CIR 140.0
S     0.0 0.0                       ! dummy surface
 ADE 2.19894; BDE 0.0; CDE 0.0
S     0.0 1398.110199               ! dummy surface
S     0.0 810.478850975
S     0.0 164.521149025             ! dummy surface near SPIRE entrance port
S     0.0 170.0                     ! dummy surface at telescope focal plane
S     0.0 0.0                       ! dummy surface at M3 mirror
S     -340.0 -180.0 REFL            !M3 spherical mirror
 BEN;  ADE -14.0; BDE 0.0; CDE 0.0
S     0.0 0.0
 ADE 28.0; BDE 0.0; CDE 0.0
S     0.0 0.0 REFL                  ! M4 scanning chopper, BDE varies from -3.964 to + 3.964 deg
 ADE 0.0; BDE 0.0; CDE 0.0
S     0.0 0.0                       !dummy surface at M4
 RET S10
S     0.0 128.83                    !dummy surface at M4
 ADE 28.0; BDE 0.0; CDE 0.0
S     -195.7179 -84.4666 REFL       !M5 toroidal mirror
 XTO;  CUX -0.00566837511493;  K   0.0; IC Yes
 A   0.0; B 0.0; C 0.0; D 0.0
 BEN;  ADE -14.0; BDE 0.0; CDE 0.0
S     0.0 -129.18322                !Re-imaged focal plane - location for 2K filter
S     0.0 100.34 REFL               !M6 flat mirror
 CCY 0;  BEN;  ADE 17.0; BDE 0.0; CDE 0.0
S     0.0 150.0                     ! cold stop location
S     -403.7387 -170.0 REFL         !M7 toroidal mirror
 CCY 0;  XTO;  CUX -0.00288079459229; CCX 0
 K   0.0; IC Yes;  A   0.0; B 0.0; C 0.0; D 0.0
 BEN;  ADE -22.0; BDE 0.0; CDE 0.0
S     0.0 198.0 REFL                !M8 flat mirror
 BEN;  ADE 22.0; BDE 0.0; CDE 0.0
SI    0.0 0.0 AIR                   !detector plane
GO
```

10.2 Sequence file REVCRY.SEQ defining the system traced from detector to space

```
RDM;LEN     "VERSION: 8.11 A      LENS VERSION: 43      Creation Date: 29-JAN-1998"
TITLE 'Reversed SPIRE for tracing from detector to space''
EPD   199.498705576
DIM   M
WL    200000.0
REF   1
WTW   1
INI   ''
CA    APE
XOB   0.0 10.5 10.5 0.0 -10.5 -10.5 -10.5 0.0 10.5    !field points at the centre,  corners and middle
YOB   0.0 0.0 10.5 10.5 10.5 0.0 -10.5 -10.5 -10.5    !of the 4 edges of the detector
VUX   0.0 0.0 0.0 0.0 0.0 0.0 0.0 0.0 0.0
VLX   0.0 0.0 0.0 0.0 0.0 0.0 0.0 0.0 0.0
VUY   0.0 0.0 0.0 0.0 0.0 0.0 0.0 0.0 0.0
VLY   0.0 0.0 0.0 0.0 0.0 0.0 0.0 0.0 0.0
SO    0.0 198.0
S     0.0 -170.0 REFL
  BEN;  ADE 22.0; BDE 0.0; CDE 0.0
S     403.7387 150.0 REFL
  CCY 0;  XTO;  CUX 0.00288079459229; CCX 0
  K   0.0; IC Yes;  A    0.0; B 0.0; C 0.0; D 0.0
  BEN;  ADE -22.0; BDE 0.0; CDE 0.0
S     0.0 100.34
  STO;  ELX L'CST' 18.98; ELY L'CST' 17.82
S     0.0 -129.18322 REFL
  CCY 0;  BEN;  ADE 17.0; BDE 0.0; CDE 0.0
S     0.0 -84.4666
S     195.7179 128.83 REFL
  XTO;  CUX 0.00566837511493
  K   0.0; IC Yes;  A    0.0; B 0.0; C 0.0; D 0.0
  BEN;  ADE -14.0; BDE 0.0; CDE 0.0
S     0.0 0.0
  ADE 28.0; BDE 0.0; CDE 0.0
S     0.0 0.0 REFL
  ADE 0.0; BDE -3.964; CDE 0.0
S     0.0 0.0
  RET S7
S     0.0 -51.23
  ADE 28.0; BDE 0.0; CDE 0.0
S     0.0 -128.77           ! 4K filter surface
S     340.0 0.0 REFL        ! M3
  BEN;  ADE -14.0; BDE 0.0; CDE 0.0
S     0.0 170.0             !dummy surface at M3
S     0.0 164.521149025     !telescope focal plane
S     0.0 108.771651        !SPIRE entrance port
S     0.0 0.0
  XDE 0.0; YDE -80.6279; ZDE 0.0
S     0.0 150.0
  ADE 2.19894; BDE 0.0; CDE 0.0
S     0.0 315.0
S     0.0 140.0
S     0.0 100.0
```

```
S     0.0 0.0
S     0.0 2373.11
  RET S14
S     0.0 0.0
S     0.0 0.0
  REV
  ADE -2.19894; BDE 0.0; CDE 0.0
S     267.82995 -1396.3648 REFL
  CON;  K   -1.2387718;  DAR
S     3046.246 3000.0 REFL
  CON;  K   -1.0
SI    0.0 0.0 AIR                    !space surface 3 metres in front of primary
ZOO   3
ZOO   EPD 199.498705576 199.498705576 199.498705576
ZOO   BDE S8 -3.964 0.0 3.964
ZOO BDC S8 100 100 100
GO
```